Final Project Report
Detailed Form

I. Title of Proposed Project:

Research and development on short distance communication and imaging for appli cations in ASEAN region

II. Project Leader:

Full name: Vo Nguyen Quoc Bao
Institution: Posts and Telecommunications Institute of Technology, Vietnam
Address: 11 Nguyen Dinh Chieu, Dakao Ward, District 1, Ho Chi Minh City, Vie tnam
Phone: +84 913 454446
E-mail: baovnq@ptithcm.edu.vn

III. Project Members:

No.	Name	Position/Degree	Department, Institution, Country	Email Address
1	Purwoko Adhi	Director/Ph.D	Research Center for Electronics and Telecommunication, Indonesian Institute of Sciences (LIPI), Indonesia	Purwoko.adhi@lipi.go.id
2	Hazim Ahmadi	Manager	Wireless Access Technology, Telkom Indonesia (TI), Indonesia	azim@telkom.co.id
3	Tuptim Angkaew	Assistant Professor/Ph.D	Chulalongkorn University (CU), Thailand	Tuptim.A@chula.ac.th
4	Vo Nguyen Quoc Bao	Associate Professor/Ph.D	Posts and Telecommunications Institute of Technology (PTIT), Vietnam	baovnq@ptit.edu.vn
5	Le Quoc Cuong	Deputy Director/Ph.D	Department of Information and Communications, People's Committee of Ho Chi Minh City (HCMC DIC), Vietnam	lequoccuong@tphcm.gov.vn
6	Tan Hanh	Vice president/Ph.D	Posts and Telecommunications Institute of Technology (PTIT), Vietnam	tanhanh@ptit.edu.vn
7	Sevia M. Idrus	Professor/Ph.D	Universiti Teknologi Malaysia (UTM), Malaysia	sevia@fke.utm.my
8	Tetsuya Kawanishi	Managing Director/Ph.D	Photonic Network Research Institute, NICT, Japan	kawanishi@nict.go.jp

9	Ukrit Mankong	Assistant Professor/Ph.D	Chiang Mai University (CMU), Thailand	ukrit.m@cmu.ac.th
10	Romli Mohamad	Department head	TM Research and development (TMRD), Malaysia	romli@tmrnd.com.my
11	Nguyen Anh Tuan	Vice director	Radio Frequency Department, the Authority of Radio Frequency Management, Ministry of Information and Communications of Vietnam (RFD), Vietnam	natuan@rfd.gov.vn
12	Joewono Widjaja	Professor/Ph.D	Institute of Science, Suranaree University of Technology (SUT), Thailand	joe_widjaja@yahoo.com
13	Duang-rudee Worasucheep	Associate Professor/Ph.D	Chulalongkorn University (CU), Thailand	Duangrudee.W@chula.ac.th

TABLE OF CONTENT

IV. Project Report 5
i. Introduction 5
ii. Project Activities 6
(1) Development and Implement 8
(2) Leveraged Resources and Participants 26
(3) Findings and Outcomes 27
(4) Broader Impact 27
(5) Future Developments 28
iii. Social Contribution 28
(1) Academic papers such as international conference, journal paper, invited paper, etc. 28
(2) Report for international standardization. 29
(3) Patent (international or domestic) 29
(4) Exhibition of the application or system the project developed 29
iv. Project conclusion 30
Appendix 32
i. CMU report 32
ii. CU report 37

LIST OF FIGURES

Figure 1 Technology map of short-distance communication and imaging technologies. ..6
Figure 2 First year activities ..6
Figure 3 Second year activities ..7
Figure 4 Third year activities ..7
Figure 5 All spectrum access radio access network (from Huawei white paper "5G: A Technology Vision) ..8
Figure 6 Examples of short-distance imaging for explosives detection ..9
Figure 7 Metro line #1 in Ho Chi Minh City. ..10
Figure 8 Stations of Metro line #1 in Ho Chi Minh City. ..11
Figure 9 Two measurement sites for the field test in Ho Chi Minh City. ..11
Figure 10 Frequency license from Vietnam RFD. ..12
Figure 11 Model for Point to Point Configuration. ..13
Figure 12 Model for measurement of reflection characteristics from walls with various incident/reflection angles. ..13
Figure 13 Model for point to point transmission of 500-Mbit/s-class data with various distances. ..13
Figure 14 Point-to-point transmission between stationary transmitter (TS-RAU) and moving receiver set on the car (TRU) ..14
Figure 15 Model for measurement of interferences received in one receiver from two transmitters with various distances. ..14
Figure 16 Multipoint-to-point transmission of 500-Mbit/s-class data. ..15
Figure 17 NICT-handmade transmitter (CW transmitter, NICT-W001 (TBD)) ..15
Figure 18 Throughput versus distance ..19
Figure 19 Received number of packets versus distance ..19
Figure 20 RSSI versus distance ..20
Figure 21 Members at PTITHCM measurement site. ..20
Figure 22 Schematic of experiments ..21
Figure 23 Expected result, i.e., Figure from New elements towards a REVISION TO RECOMMENDATION ITU-R P.1411-8 ..22
Figure 24 Transmitter NICT-W001 ..22
Figure 25 Receiver setup ..23
Figure 26 Receiver with Anritsu MS2760A-0110 ..24
Figure 27 Measurement under the ground. ..25
Figure 28 Pathloss versus distance ..25
Figure 29 Consortium structure. ..26
Figure 30 Poster at Scientific Date in Hanoi, Vietnam ..30

IV. Project Report

i. Introduction

In this project, we would like to develop new and novel technologies to realize short-distance communications and imaging technologies on both optical and radio networks and their seamless convergences, which would be useful for various applications in ASEAN region. These technologies will be important for realization of 4G and 5G mobile access networks as well as wireline access networks with high-speed and high-capacity connectivity. To form the network, in ASEAN countries, such technology is indispensable owing to complicated geographic features such as sparseness of inhabitable places: small islands, valleys in mountain area, and so on. To deliver the connectivity of the network to these areas, seamless convergence of the radio and optical technologies would be key techniques with possible low energy consumption. This project under the collaboration between the institutes in ASEAN countries is formed for feasible evaluation of the short-distance communication with the seamless convergence for the typical issues in ASEAN region. The research and development in the proposal include advanced ICT devices and/or sub-systems including demonstration, and study on possible applications for public infrastructures. We also focus on case studies and on international standardization in this region. The advanced technology can be easily adopted to the imaging technology for enhancement of civil safety and security. The integration of the communication and imaging technologies will be also discussed and evaluated.

In this project, we develop new and novel technologies to realize short-distance communications and imaging technologies on both optical and radio networks and their seamless convergences, which would be useful for various applications in ASEAN region. The R&D in the proposal include advanced ICT devices and/or sub-systems including demonstration, and study on possible applications for public infrastructures. The advanced technology can be easily adopted to the imaging technology for enhancement of civil safety and security. The integration of the communication and imaging technologies will be also discussed and evaluated.

Figure 1 show the technology map of short distance communication and imaging technologies.

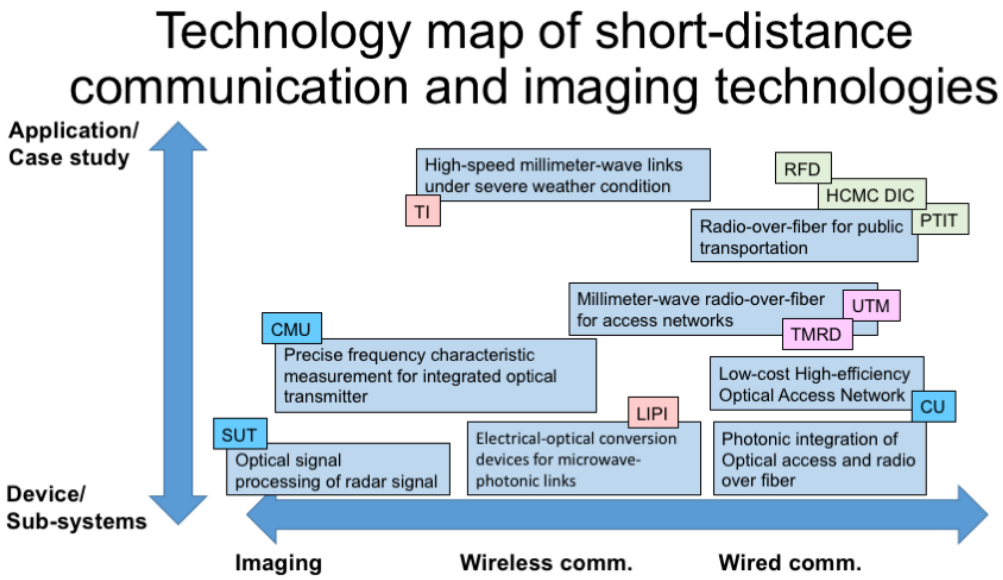

Figure 1 Technology map of short-distance communication and imaging technologies.

ii. Project Activities

Figure 2 First year activities

Figure 3 Second year activities

Figure 4 Third year activities

(1) Development and Implement

Future access communication will be relied on short-distance (<5 km) communication technology using millimeter-wave radio, free space optics, or optical fiber links to achieve cost-effective connections to end-users with high connectivity and high throughput. Future last-one-mile access technology in the mobile communication, so-called 5G, would have a throughput of 10 Gb/s to users. Thus, such high-speed communication by wireless manner would consist of millimeter-wave radio with small-cell architecture. In 5G, the small-cell configuration increases the number of base stations drastically, and in this scenario, conventional wireline technology cannot be deployed somewhere owing to its geographical or cost issues. So, high-speed and high-capacity short-distance wireless link is strongly desired in the 5G era.

All-spectrum access radio-access-network
(from Huawei white paper "5G: A Technology Vision")

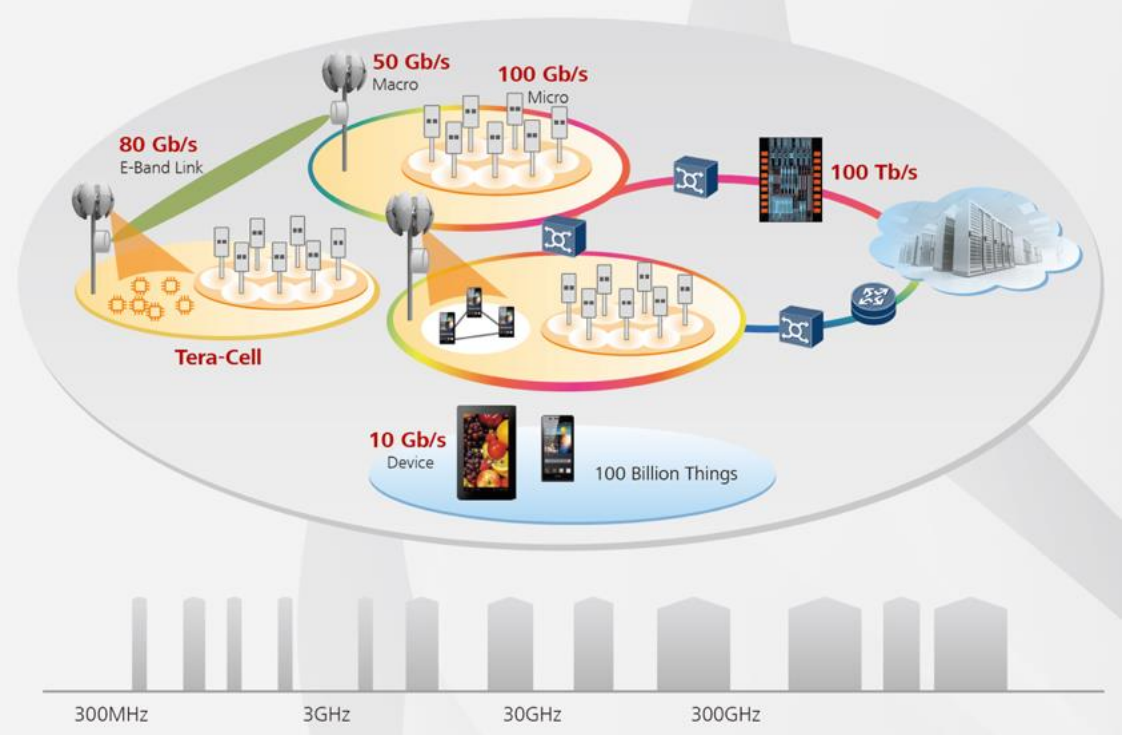

Figure 5 All spectrum access radio access network (from Huawei white paper "5G: A Technology Vision)

Moreover, seamless connectivity between a radio access network and an optical backend network will become more important to optimize the throughput and user experiences (latency). The integration of these technologies will be a key for realization of the future access network using all frequency/spectrum signals. Seamless and effective integration of the optical and radio technology on the physical layer, as well as in more upper layers, should be discussed and developed to realize the architecture in optical and radio domains with an integration of advanced devices.

In future effective network configuration, all the radio and optical signals will be handled

seamlessly on physical layer at any frequencies. In this project, the technical issues and possible solutions will be discussed.

On the other hand, enhancement of civil safety and security is desired against any incidents including terrorism attacks. Particularly in mass transportation such as aircrafts and high-speed trains, security check not only for the passenger and baggage but also for the facilities of runways and railways is effective to avoid these incidents in advance. However, current and traditional systems for inspection are not relied on standoff and real-time features; they are not convenient for users. For example, a millimeter-wave imaging technology is a candidate to obtain high-resolution images. Moreover, the material properties might be identified by the all-spectrum spectrometry; the concealed materials can be identified whether explosives or not.

In addition, the short-distance imaging technique empowered by centralized processing connected with the network has scalability on the imaging size from the small boxes to long-distance rail tracks. The centralized architecture also provides the other features such as super-resolution and computational tomography. So, the combination of the radio and optical technologies can realize the short-distance communication as well as the imaging.

Possibility of the devices, subsystems, and applications will be discussed for proof-of-concept demonstration. In addition, new paradigm for the signal processing architecture available for large-scale data will be also discussed.

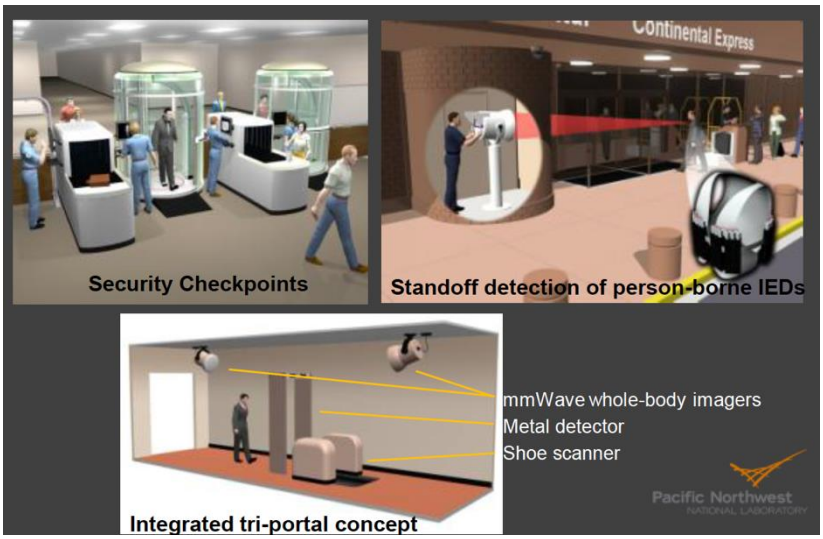

Figure 6 Examples of short-distance imaging for explosives detection
(From D. McMackin and D. Sheen presented at 2011 AAPM/COMP conf.)

Interoperability and interconnectivity will become more important for future network, which is integrated by optical and radio networks because interfaces between the optical and radio links cannot be identified accurately. In this sense, new architecture for the interface to keep the interoperability should be discussed.

In some applications, dual use for the communication and imaging might be desired: the ranging for the obstacles with information transport simultaneously in future intelligent transport systems. Advanced devices designed for the integration could be desired for the purpose with reduction of the costs. The configuration and physical properties on the devices will be discussed.

A. Trial test at Ho Chi Minh City from Jan. 2, 2017 to Jan. 11, 2017

a. Purpose

The purpose of the trial test in Ho Chi Minh City is to obverse the transmission characteristics of 90-GHz-band millimeter-wave signals under ASEAN-countries' specific conditions (squall, humidity, high temperature, etc.).

The proof-of-concept experiments of data transmission will be also performed under the situation emulated for railway radio communication system between train and trackside (RSTT).

The field trail in Ho Chi Minh City, Vietnam is from Jan. 2, 2017 to Jan. 11, 2017.

Figure 7 Metro line #1 in Ho Chi Minh City.

Figure 8 Stations of Metro line #1 in Ho Chi Minh City.

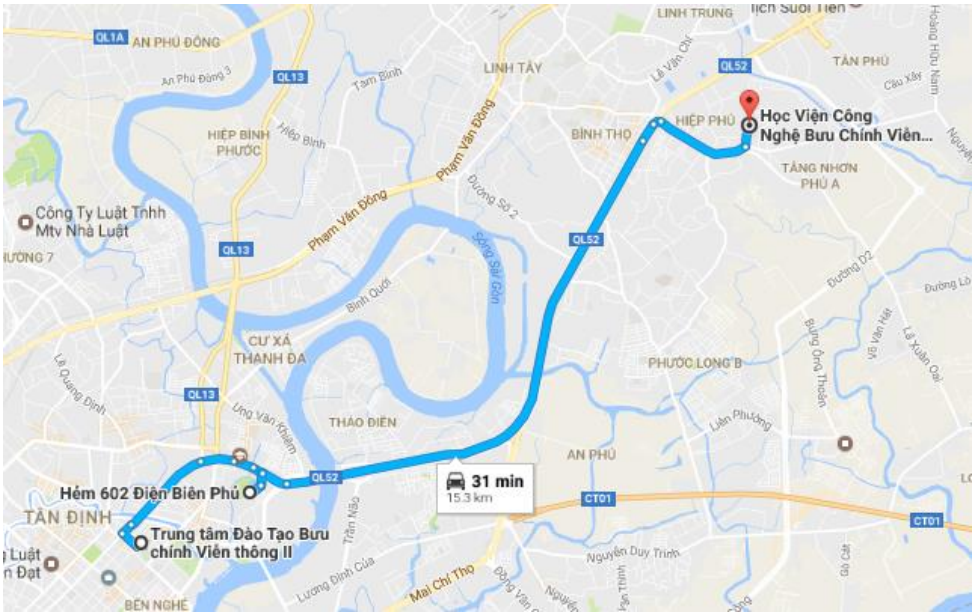

Figure 9 Two measurement sites for the field test in Ho Chi Minh City.

We consider two measurement sites including:

- **Measurement site #1:** PTIT Campus, Man Thiệ n Street, District 9
- **Measurement site #2:** Van Thanh Park (Stop #4), Dien Bien Phu Street, Binh Thanh District

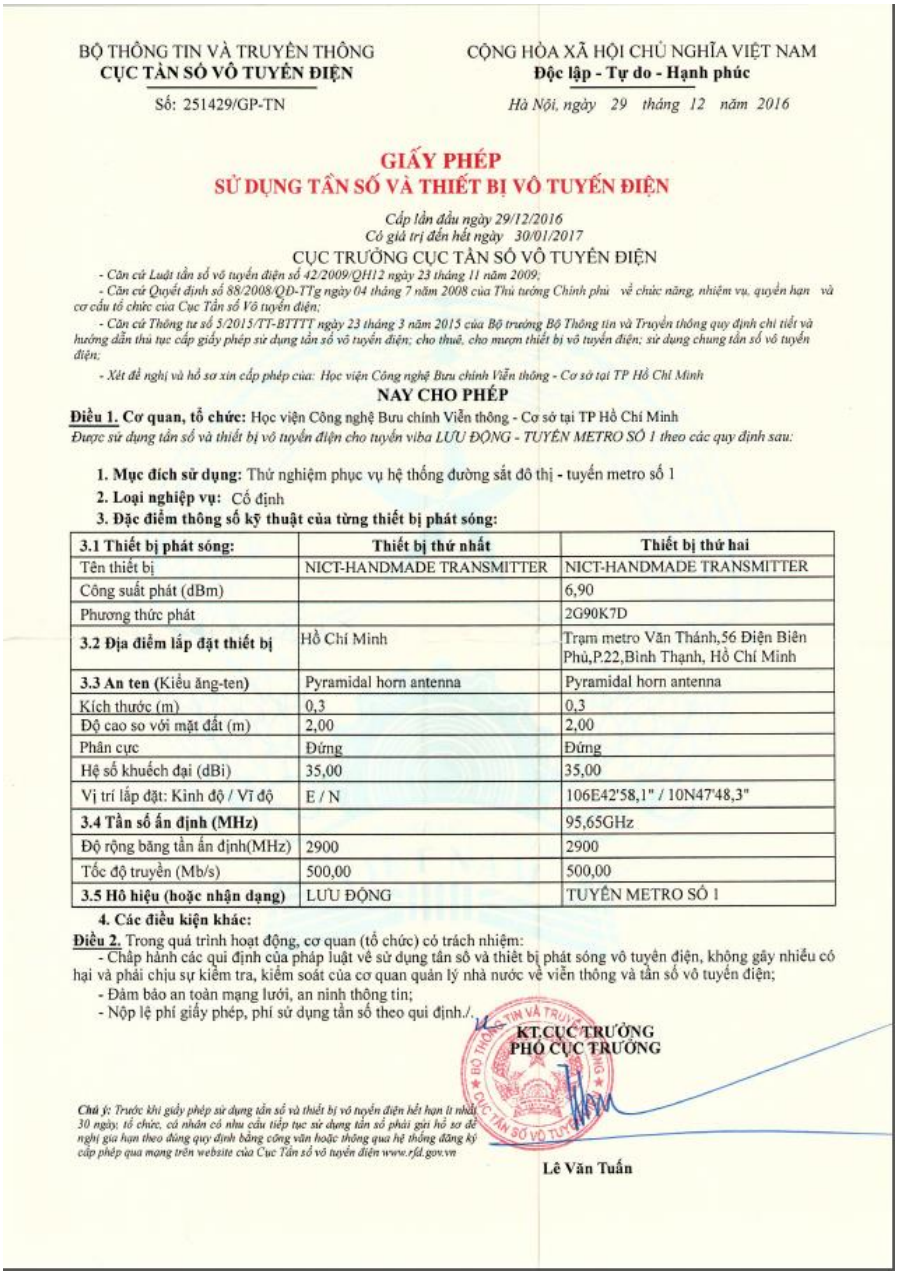

BỘ THÔNG TIN VÀ TRUYỀN THÔNG
CỤC TẦN SỐ VÔ TUYẾN ĐIỆN
Số: 251429/GP-TN

CỘNG HÒA XÃ HỘI CHỦ NGHĨA VIỆT NAM
Độc lập - Tự do - Hạnh phúc
Hà Nội, ngày 29 tháng 12 năm 2016

GIẤY PHÉP
SỬ DỤNG TẦN SỐ VÀ THIẾT BỊ VÔ TUYẾN ĐIỆN

Cấp lần đầu ngày 29/12/2016
Có giá trị đến hết ngày 30/01/2017

CỤC TRƯỞNG CỤC TẦN SỐ VÔ TUYẾN ĐIỆN

- Căn cứ Luật tần số vô tuyến điện số 42/2009/QH12 ngày 23 tháng 11 năm 2009;
- Căn cứ Quyết định số 88/2008/QĐ-TTg ngày 04 tháng 7 năm 2008 của Thủ tướng Chính phủ về chức năng, nhiệm vụ, quyền hạn và cơ cấu tổ chức của Cục Tần số Vô tuyến điện;
- Căn cứ Thông tư số 5/2015/TT-BTTTT ngày 23 tháng 3 năm 2015 của Bộ trưởng Bộ Thông tin và Truyền thông quy định chi tiết và hướng dẫn thủ tục cấp giấy phép sử dụng tần số vô tuyến điện; cho thuê, cho mượn thiết bị vô tuyến điện; sử dụng chung tần số vô tuyến điện;
- Xét đề nghị và hồ sơ xin cấp phép của: Học viện Công nghệ Bưu chính Viễn thông - Cơ sở tại TP Hồ Chí Minh

NAY CHO PHÉP

Điều 1. Cơ quan, tổ chức: Học viện Công nghệ Bưu chính Viễn thông - Cơ sở tại TP Hồ Chí Minh
Được sử dụng tần số và thiết bị vô tuyến điện cho tuyến viba LƯU ĐỘNG - TUYẾN METRO SỐ 1 theo các quy định sau:

1. Mục đích sử dụng: Thử nghiệm phục vụ hệ thống đường sắt đô thị - tuyến metro số 1
2. Loại nghiệp vụ: Cố định
3. Đặc điểm thông số kỹ thuật của từng thiết bị phát sóng:

3.1 Thiết bị phát sóng:	**Thiết bị thứ nhất**	**Thiết bị thứ hai**
Tên thiết bị	NICT-HANDMADE TRANSMITTER	NICT-HANDMADE TRANSMITTER
Công suất phát (dBm)		6,90
Phương thức phát		2G90K7D
3.2 Địa điểm lắp đặt thiết bị	Hồ Chí Minh	Trạm metro Văn Thánh,56 Điện Biên Phủ,P.22,Bình Thạnh, Hồ Chí Minh
3.3 An ten (Kiểu ăng-ten)	Pyramidal horn antenna	Pyramidal horn antenna
Kích thước (m)	0,3	0,3
Độ cao so với mặt đất (m)	2,00	2,00
Phân cực	Đứng	Đứng
Hệ số khuếch đại (dBi)	35,00	35,00
Vị trí lắp đặt: Kinh độ / Vĩ độ	E / N	106E42'58,1" / 10N47'48,3"
3.4 Tần số ấn định (MHz)		95,65GHz
Độ rộng băng tần ấn định(MHz)	2900	2900
Tốc độ truyền (Mb/s)	500,00	500,00
3.5 Hô hiệu (hoặc nhận dạng)	LƯU ĐỘNG	TUYẾN METRO SỐ 1

4. Các điều kiện khác:

Điều 2. Trong quá trình hoạt động, cơ quan (tổ chức) có trách nhiệm:
- Chấp hành các qui định của pháp luật về sử dụng tần số và thiết bị phát sóng vô tuyến điện, không gây nhiễu có hại và phải chịu sự kiểm tra, kiểm soát của cơ quan quản lý nhà nước về viễn thông và tần số vô tuyến điện;
- Đảm bảo an toàn mạng lưới, an ninh thông tin;
- Nộp lệ phí giấy phép, phí sử dụng tần số theo qui định./.

KT.CỤC TRƯỞNG
PHÓ CỤC TRƯỞNG

Lê Văn Tuấn

Chú ý: Trước khi giấy phép sử dụng tần số và thiết bị vô tuyến điện hết hạn ít nhất 30 ngày, tổ chức, cá nhân có nhu cầu tiếp tục sử dụng tần số phải gửi hồ sơ đề nghị gia hạn theo đúng quy định bằng công văn hoặc thông qua hệ thống đăng ký cấp phép qua mạng trên website của Cục Tần số vô tuyến điện www.rfd.gov.vn

Figure 10 Frequency license from Vietnam RFD.

b. Configuration for field experiment

- **CW experiment**

All the experiments will be performed under point-to-point configuration (one transmitter and one receiver).

Measurement of path loss characteristics with various transmission distance, i.e., from 0 to 100 meters.

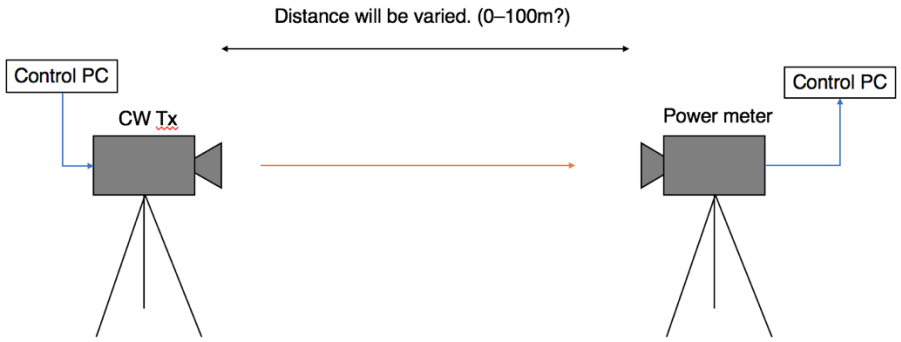

Figure 11 Model for Point to Point Configuration.

- Measurement of reflection characteristics from walls with various incident/reflection angles

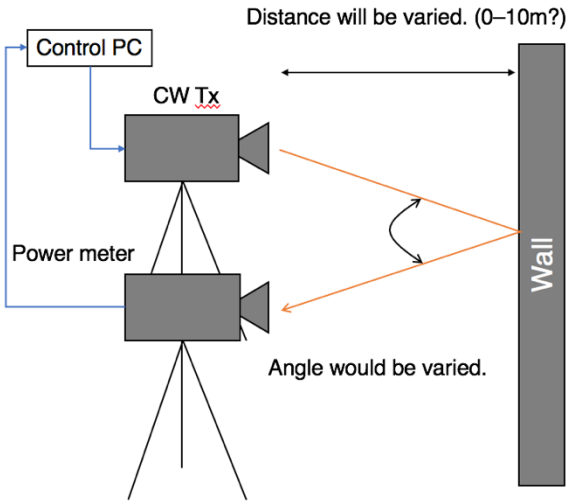

Figure 12 Model for measurement of reflection characteristics from walls with various incident/reflection angles.

- **Point-to-point transmission experiment**

All the experiments will be performed under point-to-point configuration (one transmitter and one receiver).

Point-to-point transmission of 500-Mbit/s-class data with various distances under stationary conditions.

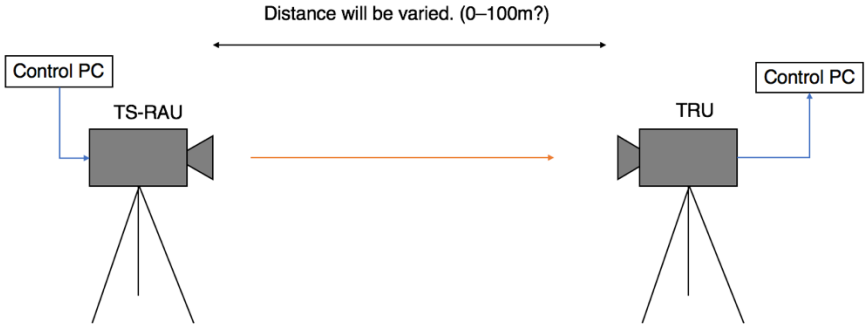

Figure 13 Model for point to point transmission of 500-Mbit/s-class data with various

distances.

Point-to-point transmission between stationary transmitter (TS-RAU) and moving receiver set on the car (TRU). The speed of the car would be less than 30 km/h.

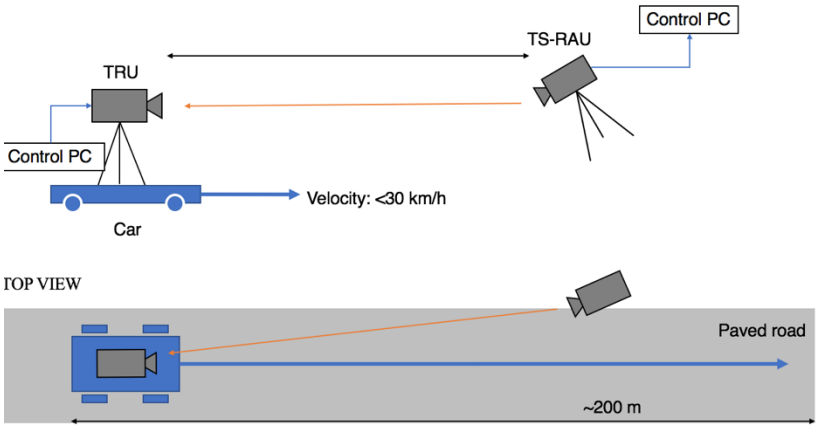

Figure 14 Point-to-point transmission between stationary transmitter (TS-RAU) and moving receiver set on the car (TRU).

- **Multipoint-to-point transmission experiment:** Measurement of interferences received in one receiver from two transmitters with various distances.

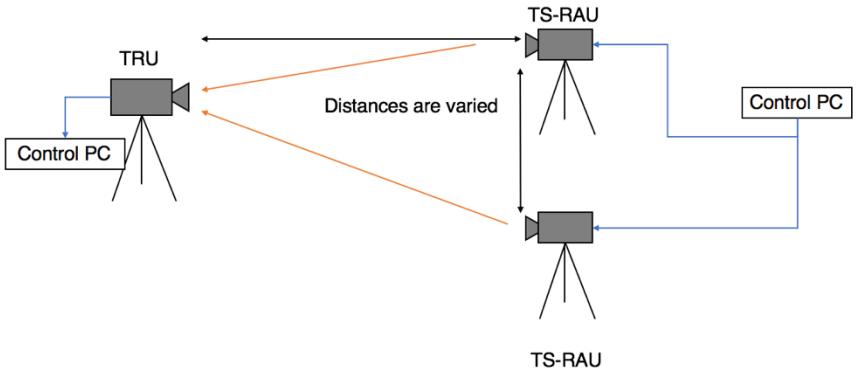

Figure 15 Model for measurement of interferences received in one receiver from two transmitters with various distances.

- Multipoint-to-point transmission of 500-Mbit/s-class data. Two transmitters (TS-RAUs) are set stationary with the separation of several 10s of meters. One receiver is moved on the car along with the TS-RAUs.

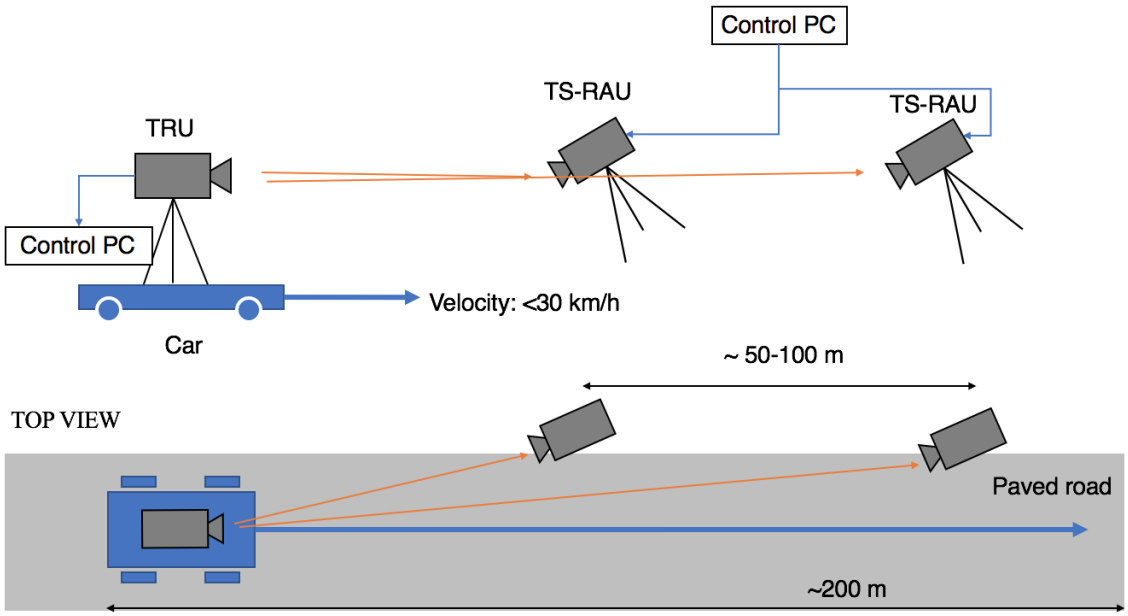

Figure 16 Multipoint-to-point transmission of 500-Mbit/s-class data.

c. *Specification of radio equipment*

- **CW experiment**

Transmitter configuration

NICT-handmade transmitter (CW transmitter, NICT-W001 (TBD)) is shown as follows.

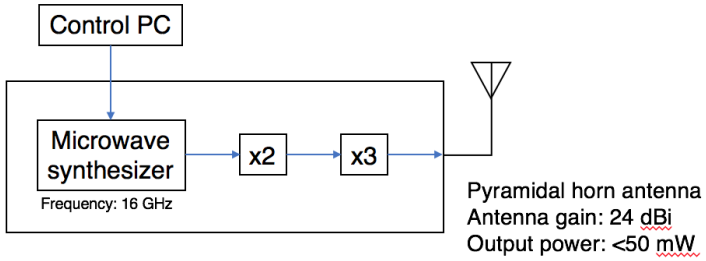

Figure 17 NICT-handmade transmitter (CW transmitter, NICT-W001 (TBD)) Radio type	CW (FM available)
Frequency range	92–96 GHZ
Output power	<50 mW
Antenna type	Pyramidal horn antenna
Antenna gain	24 dBi
Power supply	100-240Vac, 60W

Size	300mm x 210mm x 150mm
Weight	<5 kg

Receiver configuration

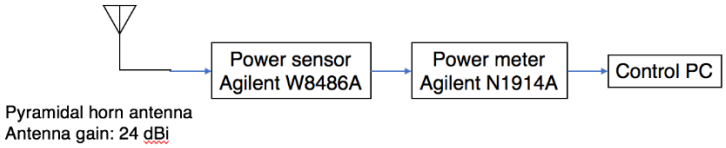

Frequency range	75–110 GHZ
Input power	1 µW–100 mW
Antenna type	Pyramidal horn antenna
Antenna gain	24 dBi
Power supply	100-240Vac, 300W

- **Transmission experiment**

Radio equipment developed by Hitachi Kokusai Electric Ltd., Japan, is based on frequency-division-multiplexed duplex system with two frequency channels (95.65 GHz and 98.45 GHz).

Transmitter configuration

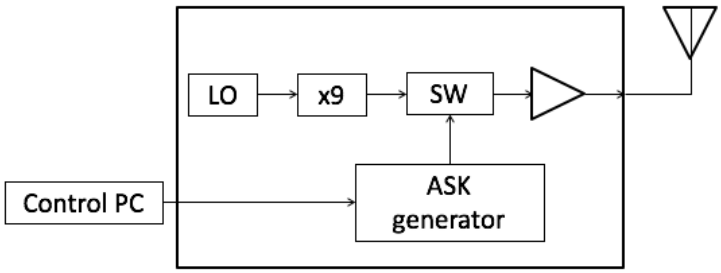

Radio type	Amplitude modulation Double sideband for data transmission
Modulation	Amplitude Shift Keying (ASK)
Data rate	Up to 500 Mbit/s

Center frequency	95.65 GHz, 97 GHZ
Occupied frequency bandwidth	2.9 GHz in each channel
Output power	<50 mW
Antenna type	Cassegrain antenna
Antenna gain	35 dBi for TRU 42 dBi for TS-RAU
Power supply	100-240Vac, <300W
Size (WDH)	TBD (TRU) TBD (TS-RAU)

Receiver configuration

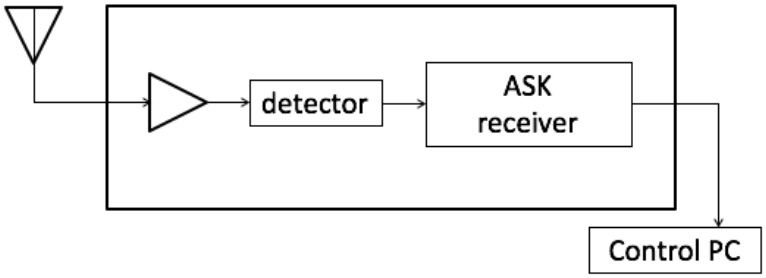

Center frequency	95.65 GHz, 97 GHZ
Frequency bandwidth	2.9 GHz in each channel
Antenna type	Cassegrain antenna
Antenna gain	35 dBi for TRU 42 dBi for TS-RAU

Frequency channel assignment

These transceivers are designed for single-frequency network, not frequency-division-multiplexing configuration. Channel 1 (center frequency of 95.65 GHz) and Channel 2 (center frequency of 97 GHz) are used exclusively in the transmission.

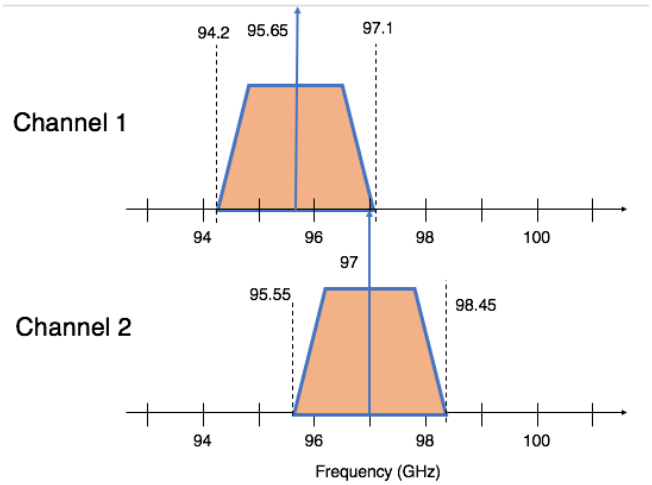

Estimated link budget: The estimation is based on the CW link provided on Table 1.

Table 1: Estimated link budget

No.	Item	Value	Unite	Note
1	Frequency	99.5	GHz	
2	Aerial power	17	dBm	50 mW
3	Tx antenna gain	30	dBi	
4	Tx feeding loss	-0.1	dB	
5	Transmitting power (at antenna)	36.9	dBm	#2+#3+#4
6	Free space path loss	-132.0	dB	1000-m transmission distance
7	Rain attenuation	0	dB	Sunny condition
8	Rx antenna gain	30	dBi	
9	Rx feeding loss	-0.1	dB	
10	Rx input power	−55.2	dBm	#5+#6+#7+#8+#9
11	Required received power (C/N)	-57.85	dBm	S/N=15dB, NF=7dB
12	System margin	2.65	dB	#10-#11

d. Tentative item list from Japan side

Table 2 provides the list of equipment supported (provided) from NICT.

Table 2 Tentative items from Japan side

No.	Items	Number
1	TS-RAU (Tx)	2 (tentative)
2	TRU (Rx)	1 (tentative)
3	NICT's CW Tx	1
4	90-GHz power meter	1
5	Tripod	3
6	Weather logger	1

7	GPS logger	1
8	Control PC	4

e. Results

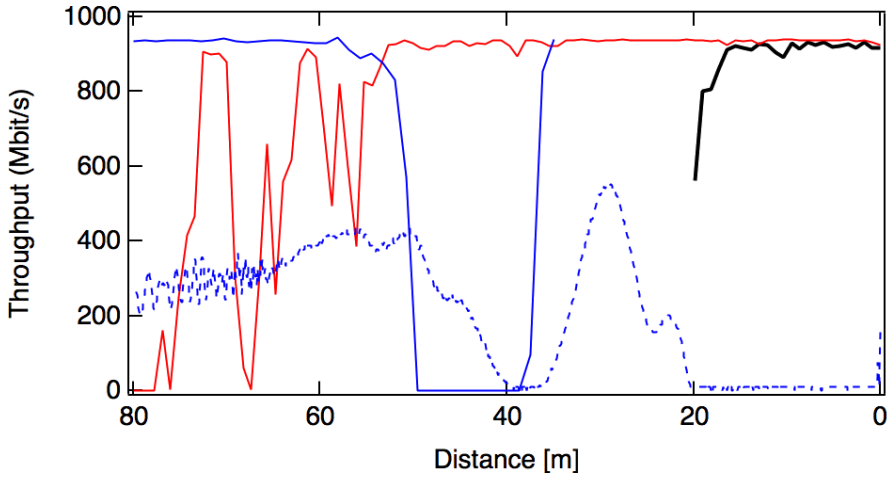

Figure 18 Throughput versus distance

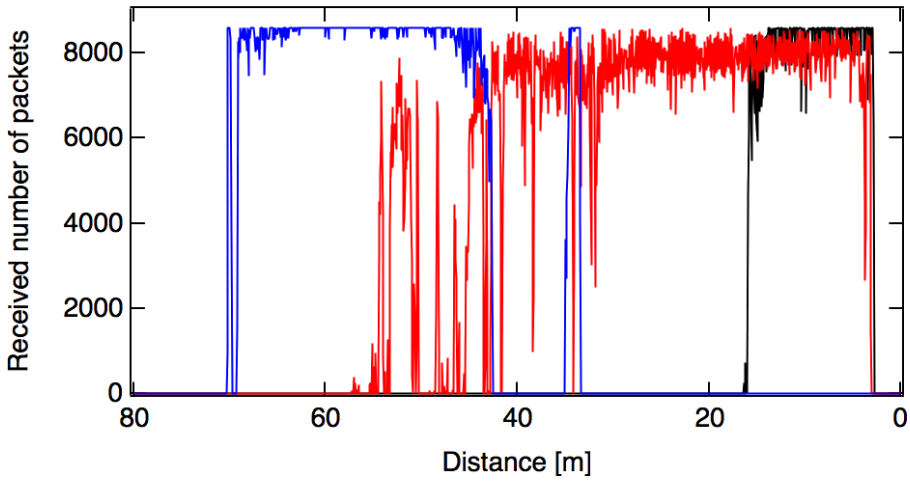

Figure 19 Received number of packets versus distance

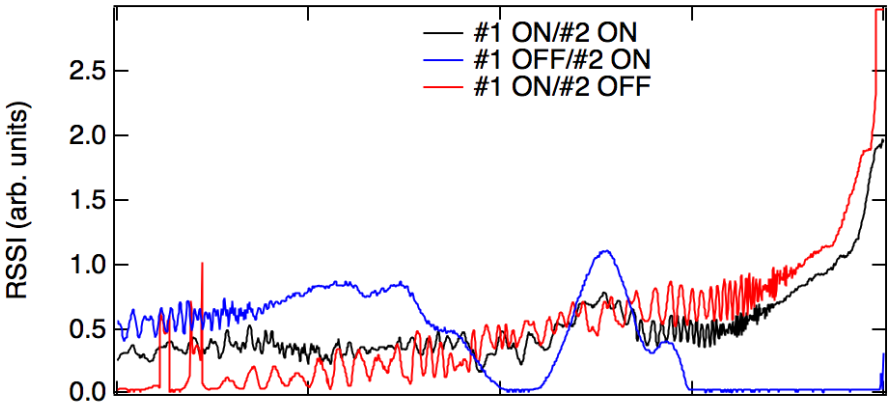

Figure 20 RSSI versus distance

- Planned experiments have been successfully done.
- The field trial clarifies issues of configuration of cells and possible suggestion for direction how to configure for railway systems.
- Also, current transceiver system is not enough for railway systems. It will be optimized and redesigned.

Figure 21 Members at PTITHCM measurement site.

B. Trial test #2 at Ho Chi Minh City from Jan. 8, 2018 to Jan. 12, 2018

a. Purpose

PTIT and NICT supported with HIKE demonstrated 1 Gbit/s link in 90 GHz band at PTIT HCMC campus and Metro Line 1 Van Tanh Park in January 2017. In the discussion, we should pursue the field trial test, which focuses on propagation characteristic measurement for clear understandings. In January 2018, radio propagation characteristics will be measured for understanding fundamental properties in the millimeter-wave bands.

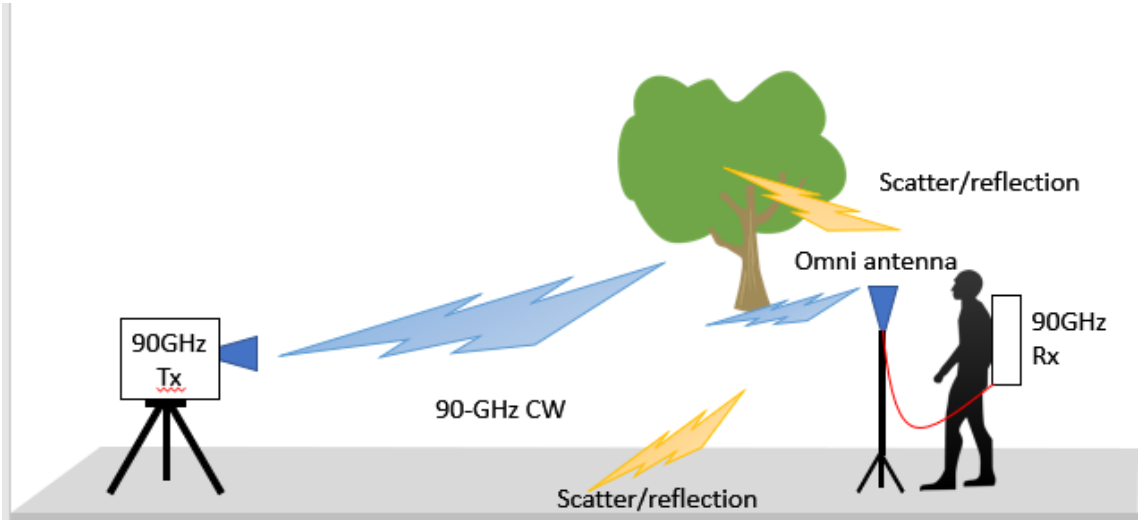

Figure 22 Schematic of experiments

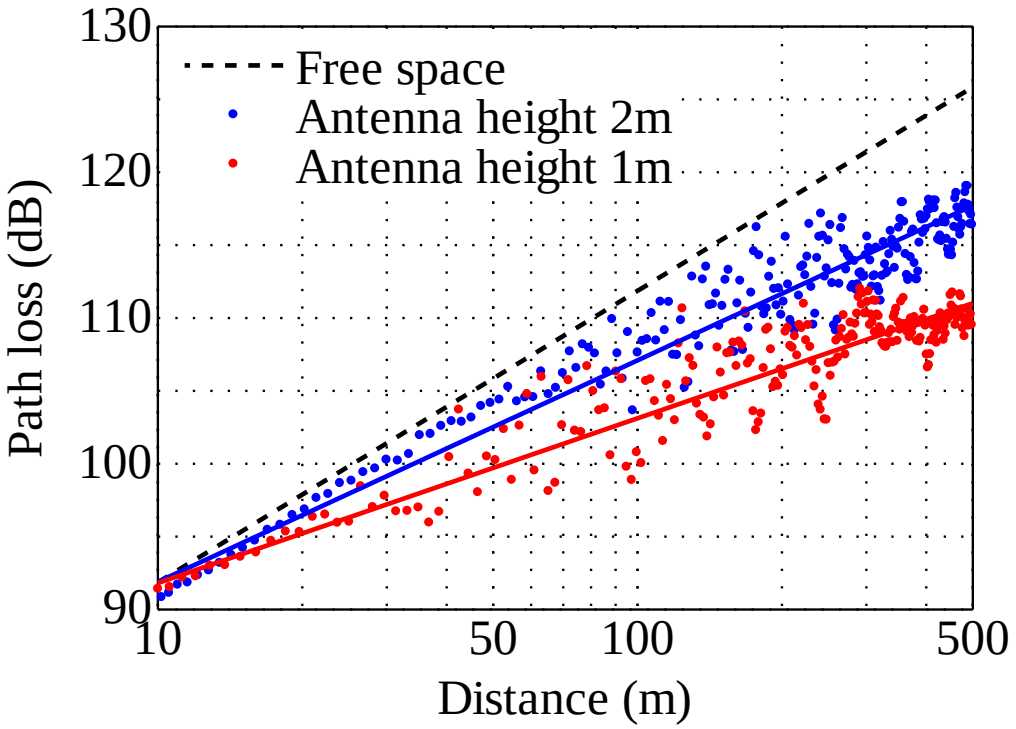

Figure 23 Expected result, i.e., Figure from New elements towards a REVISION TO RECOMMENDATION ITU-R P.1411-8

b. Setup

Figure 24 Transmitter NICT-W001.

Transmitter	(NICT-W001)

Frequency	96 GHz CW
Power	+8 dBm
Antenna	24 dBi pyramidal horn (~14deg. 3dB beamwidth)

Figure 25 Receiver setup

Figure 26 Receiver with Anritsu MS2760A-0110

The receiver is An Anritsu MS2760A-0110 using automated recording mode with GPS logger attached 360-deg omni antenna (horn antenna available). For distance measurement, we use laser range finder.

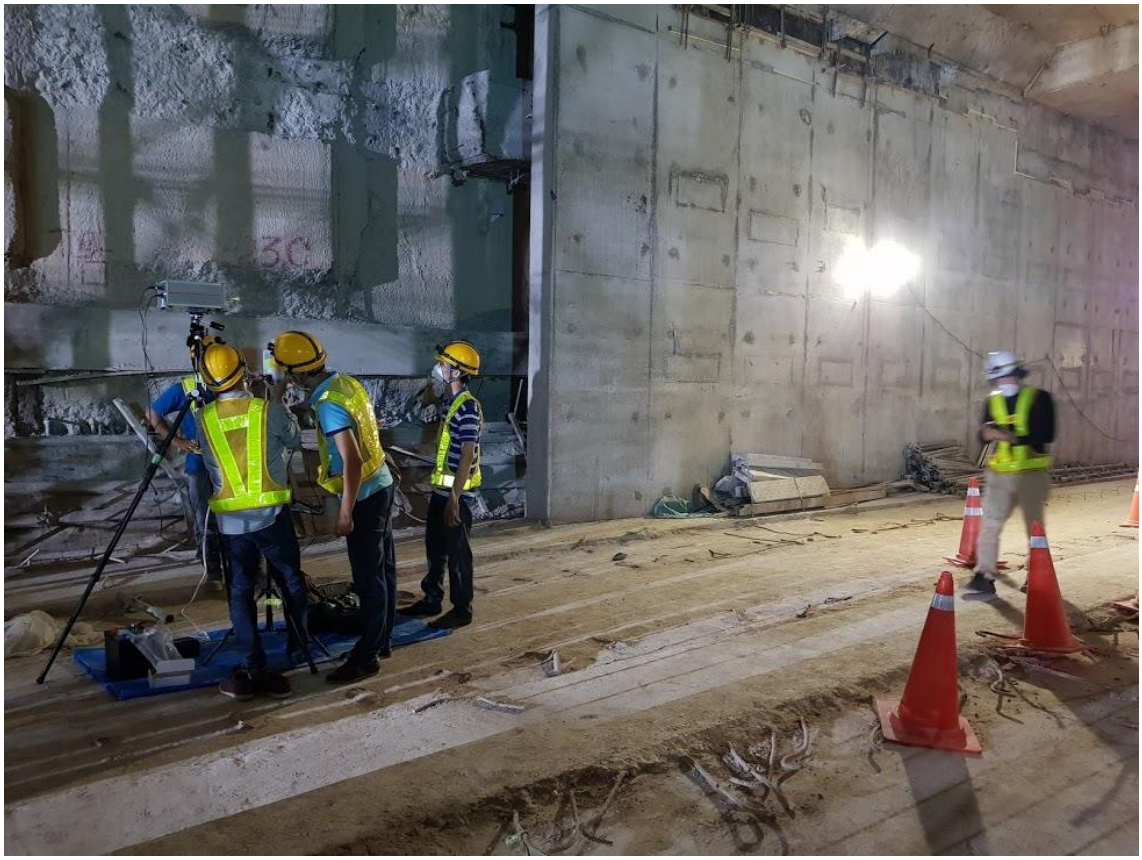

Figure 27 Measurement under the ground.

c. Obtained results

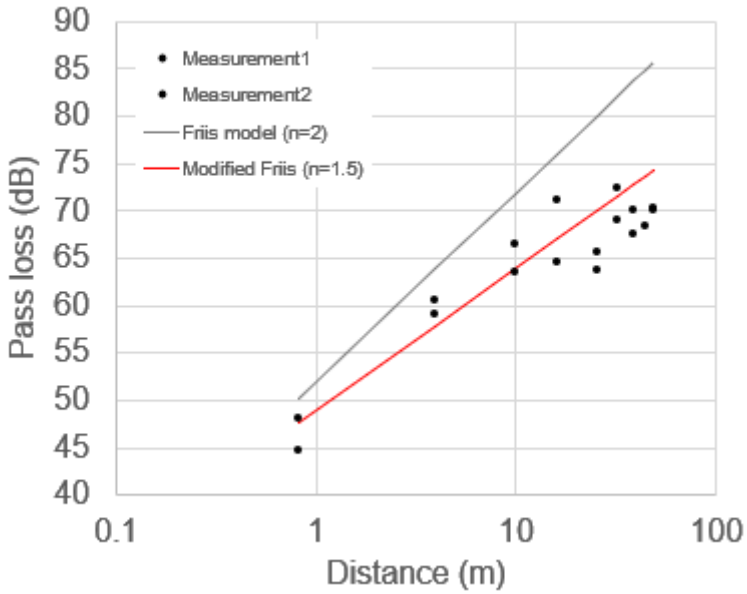

Figure 28 Pathloss versus distance

d. Summary

The trail is successful, i.e., equipment is well operated and expected results of path loss curve are also obtained.

(2) Leveraged Resources and Participants

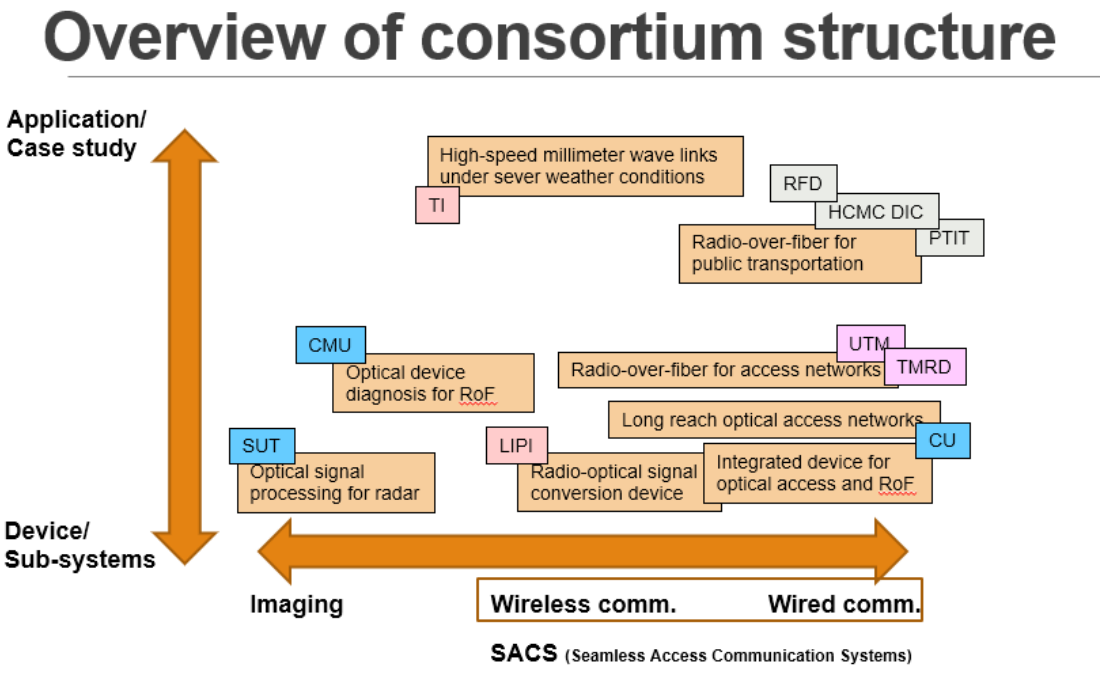

Figure 29 Consortium structure.

The R&D items that the institutes contribute in the project are as follows:

- PTIT, HCMC DIC: field trial on railway communication system
- NICT: field trial test collaborated with ASEAN institutes
- UTM, TMRD: radio over fiber system implemented to PON network (frequency subject to change)
- CMU: IQ modulation by integrated LD without any external modulator
- Chula-U: evaluation of device/subsystem with integrated optical circuits
- LIPI: optimization of E/O converter for MWP link
- TI: Survey and input to standardization bodies related on FWS under severe weather conditions

(3) Findings and Outcomes

- Measurement at distance less than 50m is available using omni-directional antenna as a receiver antenna.
- Omin-antenna has a small directivity (sensitivities are slightly different at some input angles).
- Distance greater than 50m will require a standard gain horn antenna (24 dBi) in a receiver side.

(4) Broader Impact

The effective collaboration on academies and operators helps harmonizing the fundamental research based on seeds for innovative technologies and strong demands from the operators, and finally, the institutes and governments can collaborate each other for international standardizations by these outputs.

(5) Future Developments

- Short-distance communication and imaging technologies are very potential with many future applications and networks. Their applications and performance can be improved if can be combined with other advanced technologies, such as AI and ML
- More research collaboration activities are expected to make the project cooperation more efficient, i.e., trial tests and workshops are not enough.

iii. Social Contribution

(1) Academic papers such as international conference, journal paper, invited paper, etc.

- **10 international conference papers in Flagships conferences and some technical reports**
  - [1] Atsushi Kanno, Pham Tien Dat, Naokatsu Yamamoto, Tetsuya Kawanishi, Naruto Yonemoto, Vo Nguyen Quoc Bao, Tan Hanh, Le Quoc Cuong, Kenichi Kashima, Nobuhiko Shibagaki, Radio over fiber signal generation and distribution and its application to train communication network, CLEO-PR, OECC and PGC 2017, Singapore, 2017
  - [2] P. Mekbunwan, U. Mankong, K. Inagaki, A. Kanno and T. Kawanishi, "Digital Coherent Transmitter Using Electro absorption Modulator Integrated Laser," in 2015 IEEE International Topical Meeting on Microwave Photonics (MWP), Long Beach, USA, 31 Oct – 3 Nov 2016.
  - [3] Atsushi Kanno, Pham Tien Dat, Naokatsu Yamamoto1, Tetsuya Kawanishi, "Radio over Fiber Network Technologies for Linear Cell Systems in Millimeter-Wave Bands", 2017 International Symposium on Antennas and Propagation
  - [4] Tetsuya Kawanishi, Hideki Hayashi, Keizo Inagaki, Atsushi Kanno, Naokatsu Yamamoto, "Instantaneous Frequency Measurement for Broadband Radio Signals Using Optical Single Sideband Modulation", 2017 International Symposium on Antennas and Propagation
  - [5] Nguyen Toan Van, Tran Trung Duy, Tan Hanh, and Vo Nguyen Quoc Bao, "Outage Analysis of Energy-Harvesting based Multihop Cognitive Relay Networks with Multiple Primary Receivers and Multiple Power Beacons", 2017 International Symposium on Antennas and Propagation
  - [6] Yusuf Nur Wijayanto, Yahya Sukri, Fajri Darwis, Atsushi Kanno, Hiroshi Murata, Tetsuya Kawanishi, Dadin Mahmudin, Pamungkas Daud, Purwoko Adhi, 28GHz Microstrip Yagi Antenna Stacked with Optical Modulator for 5G Wireless Communication, 2017 International Symposium on Antennas and Propagation
  - [7] Sevia Idrus, Demonstration of Receiver Generated Optical Doubinary and VSB-NRZ for Next-Generation PON, The 2017 International Symposium on Electrical and Electronics Engineering

(ISEE 201
- [8] Vo Nguyen Quoc Bao, Le Quoc Cuong, Tran Trung Duy, "A Study on WiFi Hotspot Model for Vietnam Cities" The 2017 International Symposium on Electrical and Electronics Engineering (ISEE 2017)
- [9] Atsushi Kanno, Converged Fiber-Wireless Technologies for Future Access and Radar Systems, The 2017 International Symposium on Electrical and Electronics Engineering (ISEE 2017)
- [10] Yusuf Nur Wijayanto, Atsushi Kanno, Hiroshi Murata, Tetsuya Kawanishi, Purwoko Adhi, W-Band Millimeter-Wave Patch Antennas on Optical Modulator for Runway Security Systems, 2017 IEEE Conference on Antenna Measurements and Applications, Dec. 4-6, Tsukuba, Japan

(2) Report for international standardization.

- Propose preliminary work Items on millimeter-wave radio over fiber backbone for train communication networks
- Study on Rain Attenuation Effects to millimeter wave in Indonesia: Dr. Hazim Ahmadi (in the next APT-AWG meeting)

(3) Patent (international or domestic)

None

(4) Exhibition of the application or system the project developed

- Japan Wireless EXPO' 4 May 2017, Bangkok, Thailand
- Scientific Date 18 May 2017 at Vietnam Ministry of Information and Communications

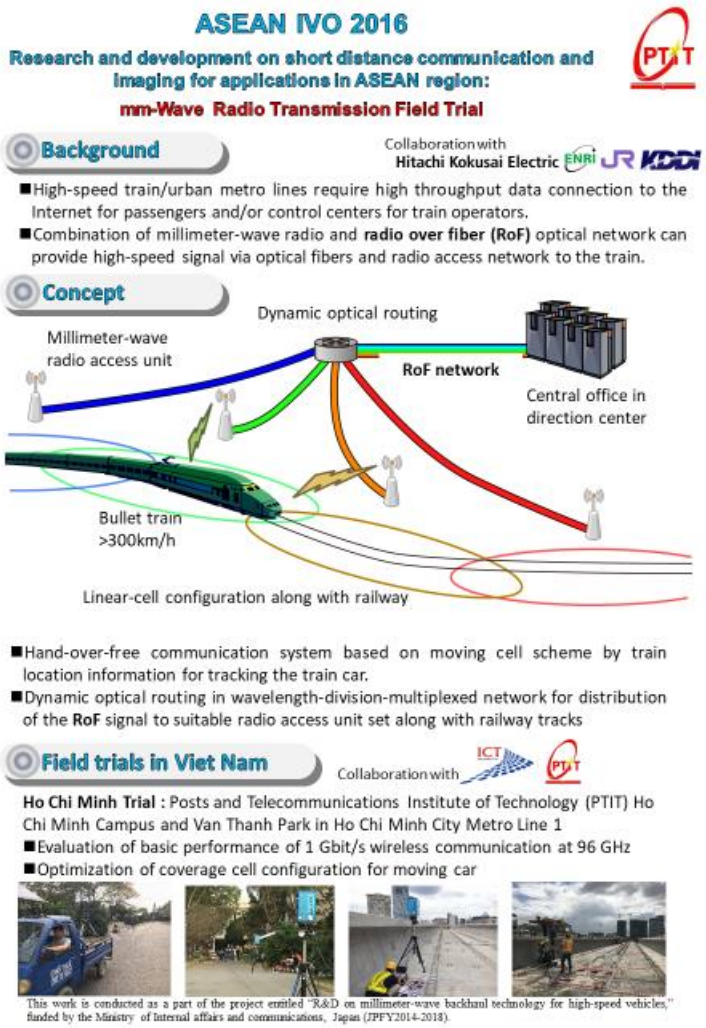

Figure 30 Poster at Scientific Date in Hanoi, Vietnam

iv. Project conclusion

- ❑Short distance communication and imaging will be the key technologies for near future communications networks and applications.
- ❑The research project has provided basic guidelines for
  - Design of photonic integrated devices
  - Millimeter-wave propagation, channelization, and its availability
  - Device evaluation technique
  - Feasibility of short-distance communication by both optical and radio technology in access networks numerically and experimentally
  - Feasibility of short-distance imaging by optical and radio, and their combination techniques
  - New hardware implementations for short-distance communication and imaging based on radio-over-fiber and its related technologies.
- ❑ The collaboration among ASEAN institutes including universities, manufactures, operators and government

- Increasing the number of research scientists, engineers in the field of the convergence of radio and optical technologies for realization of 5G networks.
- Enhancing civil security and safety by imaging as well as to increase user experiences in future networks.
- Harmonizing the fundamental research based on the seeds for innovative technologies and strong demands from the operators, and finally, the institutes and governments can organize for international standardizations by these outputs.

Appendix

i. CMU report

Precise frequency characteristic measurement for integrated optical transmitter

by Dr. Ukrit Mankong (CMU), Mr. Praimet Mekbungwan (CMU), Dr Keizo Inagaki (NICT)

In 2016, we have carried out the research on frequency characteristics of phase and amplitude modulation of electroabsorption modulator integrated laser (EML) and attempted preliminary modulation experiment on the EML. We have the following publication.

- P. Mekbunwan, U. Mankong, K. Inagaki, A. Kanno and T. Kawanishi, "Digital Coherent Transmitter Using Electroabsorption Modulator Integrated Laser," in 2015 *IEEE International Topical Meeting on Microwave Photonics (MWP)*, Long Beach, USA, 31 Oct – 3 Nov 2016.

In the 2nd year of project we will improve the modulation scheme of EML to achieve the desired results.

***Abstract*—We investigate the feasibility of an electroabsorption modulator integrated laser as a digital coherent transmitter. The laser and EAM sections are used as phase and amplitude modulators respectively. We discuss the challenges involved and demonstrate the combined phase and amplitude modulation on a commercial device.**

Keywords—electroabsorption modulator; digital coherent; phase modulation; chirp, frequency response

I. INTRODUCTION

Future transceiver technology for both optical access and radio over fiber (RoF) system is moving towards a smaller form-factor module. We are seeing new device designs where both optical modulator and laser are integrated. Moreover, digital coherent technologies for optical transmission and RoF systems have been proposed to achieve better spectral efficiency and sensitivity [1]. Typical IQ modulator in such system is a nested modulator or a dual parallel machzender Mach-Zhender modulator used as a discrete device. This type of modulator is based on $LiNbO_3$, which cannot be integrated to a light source. Thus an electro-absorption modulator integrated laser (EML), currently used for intensity modulation, is also a candidate for this purpose, capable of up to 10 Gbaud/s rate.

In this work we demonstrate the feasibility of Quadrature Amplitude Modulation (QAM) using EML, which consists of laser diode (LD) and electroabsorption modulator (EAM) sections. Using an EML for advanced modulation means that phase and intensity of light are separately modulated by the laser and EAM section as in Fig. 1. Hence frequency characterizations of amplitude and phase response of both laser and EAM are crucial. There have been several techniques to measure modulation responses of transmitters and modulators [2-5]. We have also previously developed a method to obtain induced phase response due to amplitude modulation, or chirp, for arbitrary baud rate using coherent detection technique with digital signal processing [6-7]. The similar technique can be applied to measure phase response of a modulated laser and the induced amplitude change due to phase modulation.

In the experiment, we use a commercial EML device to demonstrate a potential for QAM modulation where both laser and EAM sections are modulated. The device has only been designed for intensity modulation. Therefore the low bandwidth of the laser biasing port limits the data frequency for direct modulation. However the method should apply to higher baud rate if high frequency signal ports are to be made available to both the laser and EAM sections.

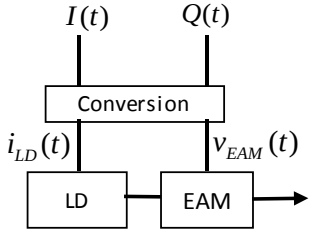

Fig. 1: Advanced modulation of EML

I. Device Frequency Characterization

A. *Amplitude and phase response of the transmitter*

From the schematic in Fig. 1, advanced modulation is achieved by sequential phase and amplitude modulations to the laser and electroabsorption modulator sections of the integrated EML respectively, using the signals converted from in-phase and quadrature signals. However either laser or EAM is a true phase or amplitude modulator. Precise characterizations of the devices are required so that appropriate signal pre-compensation may be applied. The following subsections summarize the techniques and the important results.

B. *Frequency characteristics of induced phase response of the EAM section due to intensity modulation*

Amplitude modulation response of an E/O device may be conveniently measured by a lightwave component analyzer. An alternative method would be using a two-tone light technique generated by a high-ER MZM [2] or a standard MZM to firstly obtain the response of an O/E device and subsequently of an E/O device [3,4] The induced phase error due to amplitude response or chirp of a modulator may be measured by a vector space method using coherent detection with digital signal post-processing [6,7]. The method is useful as frequency characteristics of chirp can be obtained, this method is used to measured chirp characteristics of integrated EAM as shown in Fig. 2. Chirp of an intensity modulator has an effect on the constellation diagram as shown in Fig.3, where phase of the sampled signal changes with amplitude. In addition, the time domain chirp variation can be measured by such method and is useful to implement the I-Q conversion step in the proposed scheme.

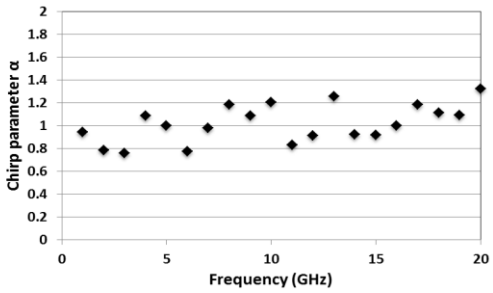

Fig. 2: Frequency characteristics of EAM chirp

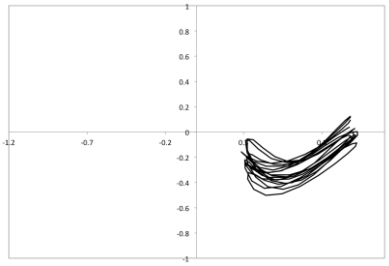

Fig. 3 Measured chirp effect in vector space

C. *Frequency characteristics of induced amplitude response of the laser diode section due to phase modulation*

We can also apply the similar vector space method [6,7] to obtain both phase response and induced amplitude response at arbitrary frequencies. The results of induced amplitude response is shown in Fig. 4. The proportional amplitude change is defined here by the ratio of amplitude change to the normalized signal amplitude for $\pm\pi/2$ phase modulation (total π radians). The effect of induced amplitude response on the constellation diagram is shown in Fig. 5. Phase noise causes drift in the total π and we observe significant amplitude differences at 0 phase. The constellation can be understood by the time variation of induced amplitude modulation depicted clearly in Fig. 6. The dotted curved is the phase modulation in radian (using right hand axis). The solid curved is the induced amplitude (using left hand axis) where the results show that the amplitude change is also sinusoidal and is phase shifted from the phase modulation.

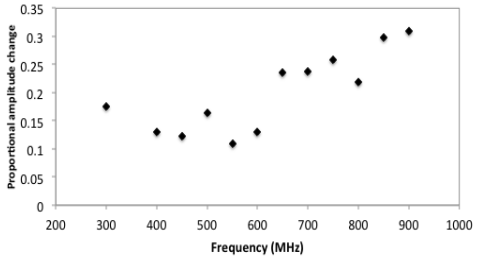

Fig. 4: Frequency characteristics of Laser induced amplitude change to π phase peak-to-peak modulation

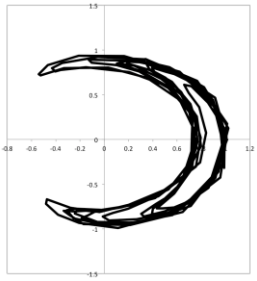

Fig. 5 Measured constellation of laser section phase modulated signal

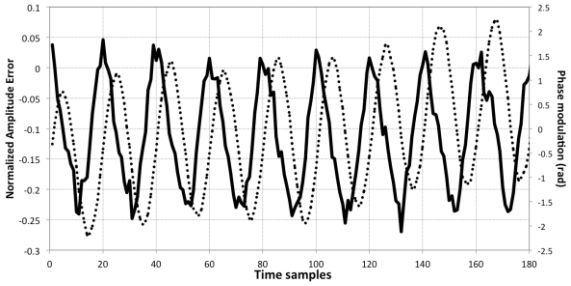

Fig. 6 Time domain phase (dotted) and induced amplitude (solid) modulation of the laser section

I. DEMONSTRATION OFCOMBINED PHASE AND AMPLITUDE MODULATION OF AN EML, INCLUDING RESULTS AND DISCUSSIONS

The standard method for QAM modulation is by modulation of the in-phase and the $\pi/2$ shifted optical carriers. In our scheme, they should be converted to amplitude and phase signals. modulation is achieved by applying both amplitude and phase modulating signals ($v_{EAM}(t)$ and $i_{LD}(t)$ respectively) to the EML as shown in Fig. 7. The output is analysed by mixing it with external LO signal from a tunable laser, using a Keysight optical modulation analyser. The resulting constellation is also depicted in the same figure at 700Mbaud/s. Note that the rate is limited since the laser modulating signal is applied by soldering to the only available DC connector. Higher rate is feasible if the high frequency signal ports are made for the laser as well as the EAM section. result is not true 4QAM since the diagonal (π phase) transition is not realized due to limitation of EAM extinction ratio. Thus it can be considered as $\pi/2$ BPSK modulation:

Optical phase modulation, then amplitude modulation are achieved sequentially. If only $i_{LD}(t)$ is applied, we obtain such curved symbol transition as in Fig. 8(a) as optical phase is changed by $\pi/2$, noting the accompanying amplitude change. Hence $v_{EAM}(t)$ is applied to compensate for the amplitude to the EAM part of the EML at twice the $i_{LD}(t)$ frequency for both up and down phase change. Almost straight symbol transition as in Fig. 8(b) is achieved, which is the preferred transition, wh ere in Fig. 8(c) the mismatched phase of $i_{LD}(t)$ and $v_{EAM}(t)$ causes the sub-optimal symbol transition. This result is only of the simple amplitude compensation. To improve the modulation scheme we must apply the

chirp characteristics and the induced amplitude/phase modulation in section II as well as adaptive digital filtering technique to the modulating signal.

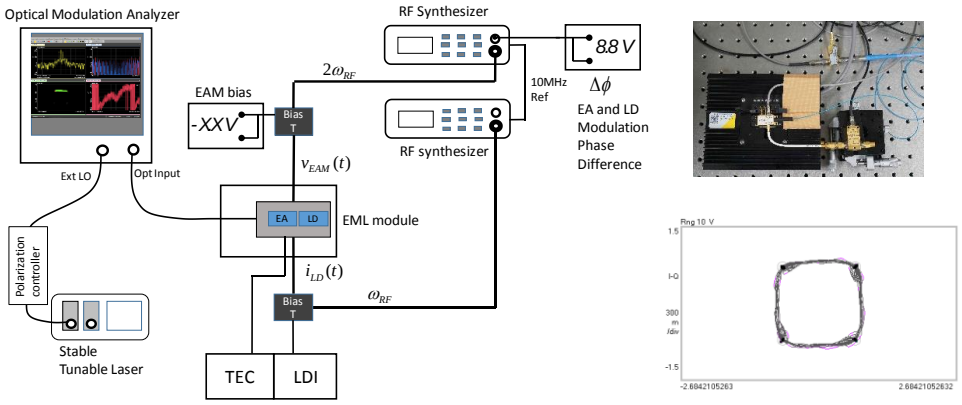

Fig. 7: Experiment setup for $\pi/2$ BPSK modulation of EML

(a) Only phase modulation (b) amplitude compensated (c) suboptimal compensation

Fig. 8: Example of transition between adjacent symbols

I. CONCLUSION

We have demonstrated advanced amplitude and phase modulation of optical signal by electro-absorption modulator integrated laser. Phase and amplitude of light are modulated sequentially to achieve the desired format. The advantage of this modulation method is the integrability and size, thus having potential in digital coherent transmission. However the extinction ratio of EAM We use a EML with only one high speed connector to the EAM, thus our homemade connection of the laser section limits the bandwidth as well as the achievable baud rate. New packaging design to introduce high speed connector to the LD bias should increase the speed up to the order of 10Gb/s

REFERENCES

[1] K. Kitayama, A. Murata, and Y. Yoshida, "Digital Coherent Technology for Optical Fiber and Radio -Over-Fiber Transmission Systems,' J. Lightwave Technol., vol. 32, no. 20, pp 3411-3420, 2014.

[2] K. Inagaki and T. Kawanishi, "Calibration method of optoelectronic frequency response using Mach-Zehnder modulator," in Microwave Photonics (MWP), IEEE Topical Meeting on, 2010, pp. 143-146.

[3] S. Potha, N. Siripon, U. Mankong, K. Inagaki and T. Kawanishi, "Simple directly modulated laser diode frequency characterizat ion using calibrated PD by two-tone light MZM method," in Proc. MWP/APMP 2014, pp. 237-239.

[1] T.Tangmala, S.Potha, U.Mankong, K.Inagaki, and T. Kawanishi, "Optoelectronic frequency response measurement using standard Mach-Zehnder modulator," in Proc. ICOCN 2012, Pattaya, Thailand, 2012.

[2] F. Devaux, Y. Sorel, and J. F. Kerdiles, "Simple Measurement of Fiber Dispersion and of Chirp Parameter of Intensity Modulate d Light Emitter," J. Lightwave Technol., vol. 11, no. 12, pp. 1937-1940, 1993

[3] U. Mankong, T. Tangmala, K. Inagaki, A. Kanno and T. Kawanishi, "Direct chirp measurement of electro absorption modulator using optical homodyne quadrature demodulation technique," in Proc. ECOC 2014, paper P.2.15, 2014

[4] •U. Mankong, P. Mekbunwan, K. Inagaki, A. Kanno and T. Kawanishi, "Dynamic small-signal chirp characteristics of external and integrated modulators," in 2015 IEEE International Topical Meeting on Microwave Photonics (MWP), Paphos, Cyprus, 26 -29 October 2015.

ii. CU report

Low-cost High-efficiency Optical Access Network

by Dr. Duang-rudee Worasucheep, Miss Budsara Boriboon and Mr. Suchaj Rakkammee

Many optical amplifiers are installed to boost small signals, mainly in fiber backbone networks such as intercity links, transcontinental and submarine cables. Their applications are shown in Fig. 1 [1]: (1) *In-line amplifier* to increase transmission distance, (2) *Preamplifier* to improve receiver's sensitivity, (3) *Booster* to increase transmitter's power, and (4) *Local Area Network (LAN) Booster* to compensate coupler's loss. The first 3 cases of point-to-point links aim to increase their total lengths between transmitters and receivers, whereas the last case of star links aims to have many receivers. The more splitting ports at star coupler will require a larger gain amplifier.

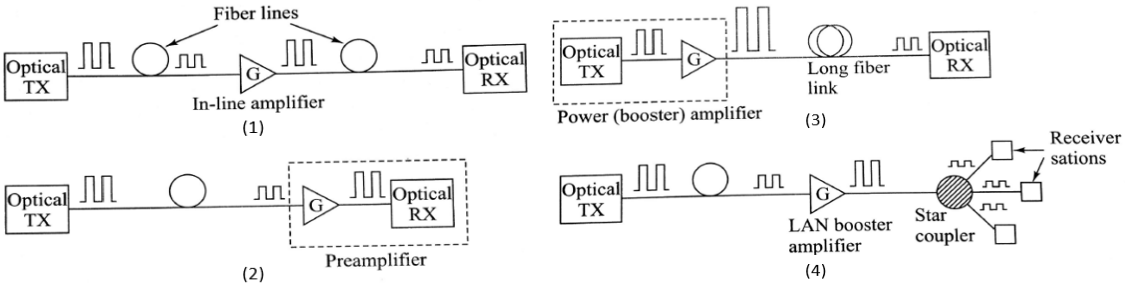

Figure 1 Applications of Optical Amplifiers. [1]

Basically, the optical amplifiers are classified into 3 types based on technology: (1) Erbium Doped Fiber Amplifier (EDFA), (2) Semiconductor Optical Amplifier (SOA), and (3) Fiber Raman amplifier. In our research on optical access network, which has the standard upstream and downstream transmission wavelengths, we will focus only on EDFA and SOA due to their appropriate operating wavelengths.

EDFA consists of 10-30 meter of optical fiber [1] with core-doped by Erbium element to amplify input signal between 1530 nm and 1560 nm wavelengths, also known as C-band. EDFA uses high-power lasers at 980 nm or/and 1480 nm wavelengths as optical pumping. These pump lasers excite electrons in lower energy band up to higher energy band. When they return to lower energy band, the desired photons are emitted as amplified output, as shown in Fig. 2 Stimulated emission. Typically, EDFA is used in long-haul WDM (Wavelength Division Multiplexing) links. In the access networks, we use EDFA operating at 1550 nm and 1577 nm wavelengths for downstream transmissions according to the ITU-T G.983.3 [2] and G.987 [3] standards respectively.

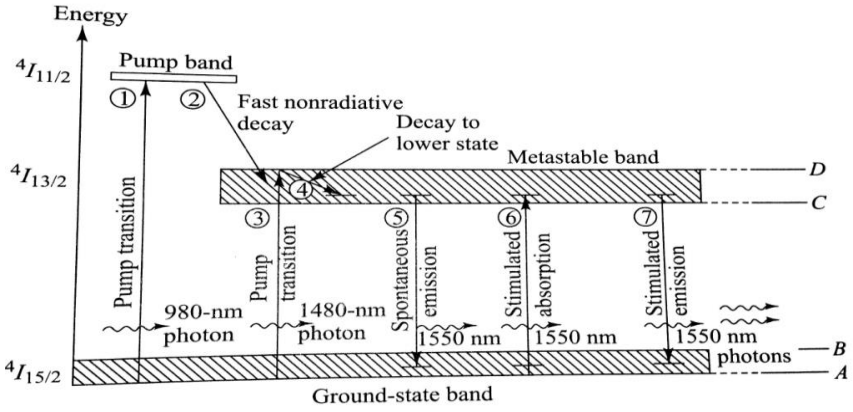

Figure 2 Electron Transitions in EDFA's Energy Bands. [1]

SOA has the same structure as a Fabry-Perot laser [1], but with antireflection coating on both sides of structure as shown in Fig. 3. Its pump current causes population inversion having more electrons in higher energy band. Then, the stimulated emission generates desired photons. Unlike EDFA that works only in C-band, SOA can amplify various input wavelengths based on different doped elements. For example, SOA doped with InGaAsP works over a wide range of O-band to U-band. In the access networks, we use SOA operating at 1310 nm and 1277 nm wavelengths for upstream transmissions according to the ITU-T G.984.2 [4] and G.987 [3] standards respectively.

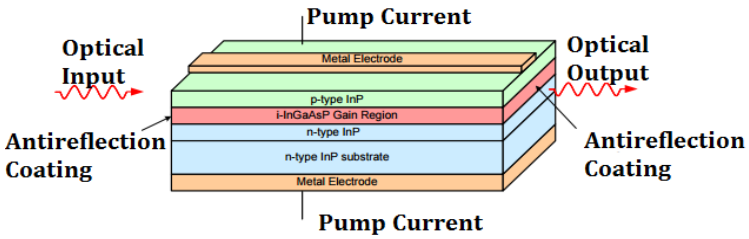

Figure 1 SOA Structure. [5]

At present, the Passive Optical Network (PON) is quite popular with high bitrate, based on G-PON and XG-PON standards from ITU-T at nearly 2.5 Gb/s and 10 Gb/s respectively. To extend coverage area as in Fig. 4 (a) and increase a number of users as in Fig. 4 (b), the optical amplifiers must be included in these PONs for both rural area and metro area respectively. Consequently, PON becomes optical access network.

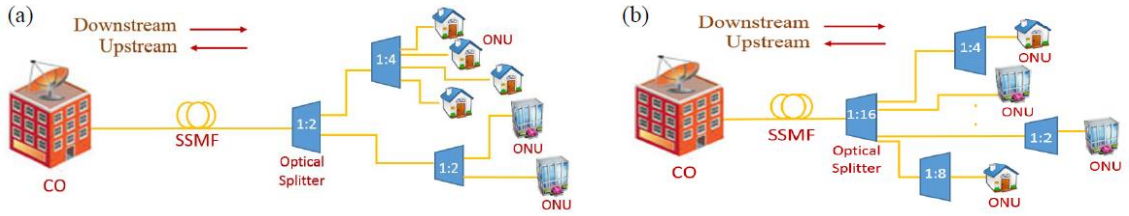

Figure 2 Access networks: (a) Rural area with long SSMF and (b) Metro area with a large number of users.

This access network has downstream and upstream transmissions, so the bidirectional optical amplifier is required. For instance, the research by Shimizu et al. in 2014 successfully demonstrated 0.73-W extremely low-power-consumption optical amplifier repeater for 10G-EPON systems [6].

In this research, first we study the characteristics of EDFA and SOA. Next, the downlink transmission using an EDFA and uplink transmission using a SOA will be tested separately. Finally, the 10 Gb/s access network using bidirectional optical amplifier will be experimented to measure power budget and Bit Error Rate (BER) at different combinations of SSMF's lengths and a number of splitting ports.

For this progress report, we already study 3 optical amplifiers as follows:

- EDFA from VIAVI [7]

- EDFA from Amonics [8]

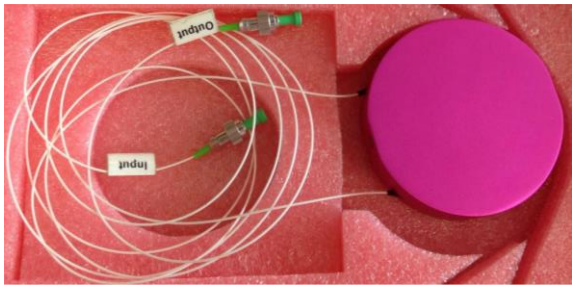

- SOA from Amonics [9]

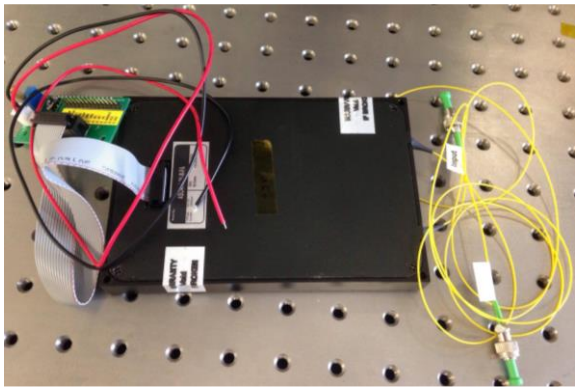

Experimental results of EDFA (VIAVI)

1. Gain (dB): we use Optical Spectrum Analyzer (OSA) (Yokogawa, AQ6370D) [10] to measure both the input powers (P_{in}, dBm) and output powers (P_{out}, dBm) of EDFA at 1550 nm wavelength, as in Fig. 5 block diagram. The gain (dB) is a power difference between output and input. The results are shown in Fig. 5 at 50% and 100% EDFA's laser currents. Obviously, this gain depends on laser current. For example, at input power P_{in} = -20 dBm, the EDFA gain is 25 and 35 dB at 50% and 100% laser currents respectively. Additionally, the smaller input power will get a larger gain.

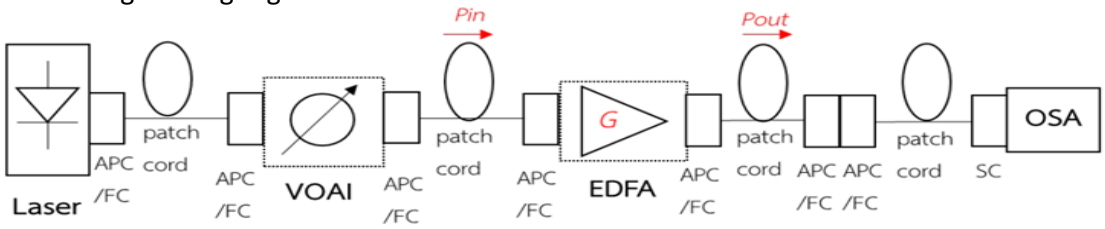

- EDFA from Amonics [8]

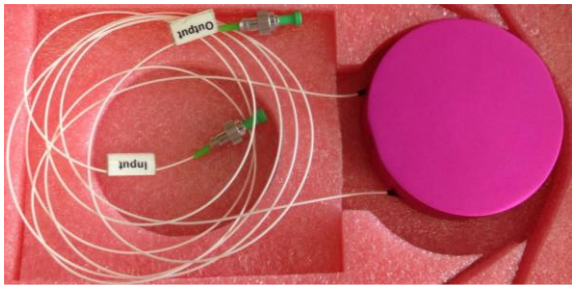

- SOA from Amonics [9]

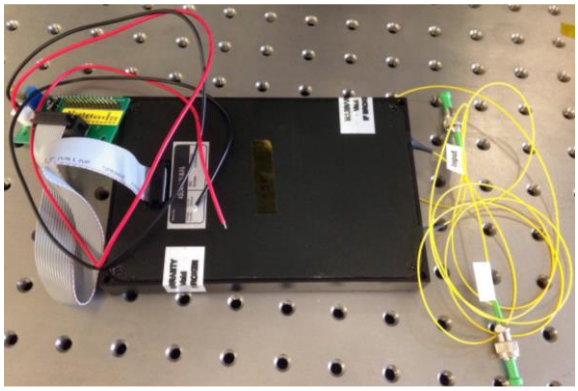

Experimental results of EDFA (VIAVI)

1. Gain (dB): we use Optical Spectrum Analyzer (OSA) (Yokogawa, AQ6370D) [10] to measure both the input powers (P_{in}, dBm) and output powers (P_{out}, dBm) of EDFA at 1550 nm wavelength, as in Fig. 5 block diagram. The gain (dB) is a power difference between output and input. The results are shown in Fig. 5 at 50% and 100% EDFA's laser currents. Obviously, this gain depends on laser current. For example, at input power P_{in} = -20 dBm, the EDFA gain is 25 and 35 dB at 50% and 100% laser currents respectively. Additionally, the smaller input power will get a larger gain.

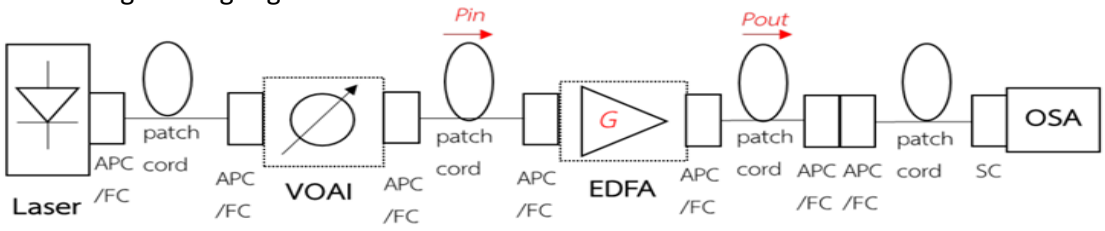

Next, we set a tunable laser in Fig. 5 block diagram to output seven wavelengths: 1540.953, 1543.929, 1549.917, 1549.916, 1552.927, 1555.949 and 1558.983 nm. The spectral profiles of equal powers are shown in Fig.7 (a). Then, we attenuate these wavelengths by 0, 10, 20, 30, 40, 50 and 60 dB respectively. Hence, their corresponding profiles are shown in Fig.7 (b) as the input into EDFA.

(a) (b)

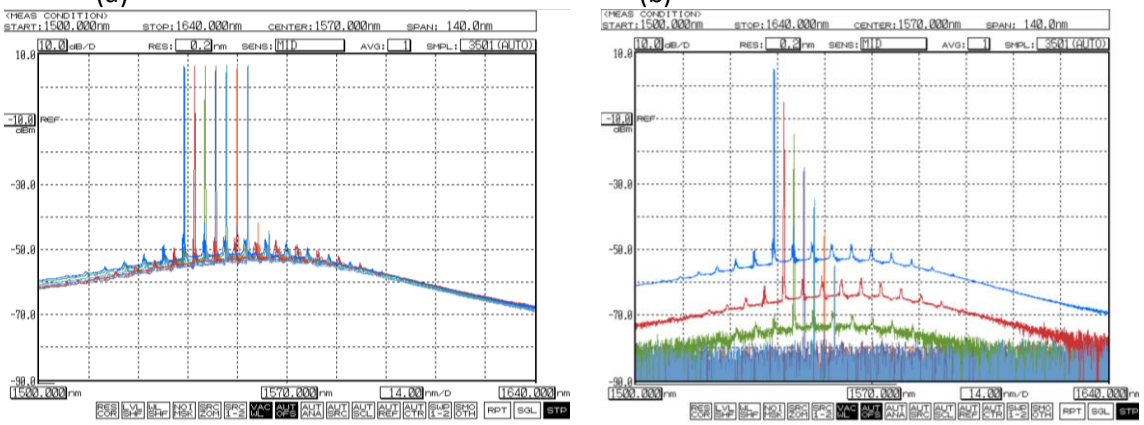

Figure 1 Spectral profiles of 7 input wavelengths: (a) equal powers and (b) attenuated powers into EDFA (VIAVI)

The output spectral profiles of EDFA (VIAVI) with seven attenuated input wavelengths are shown in Fig. 8 (a) and (b) at EDFA laser current of 10% and 50% respectively. Comparing the results in Fig. 7 (b) and Fig. 8 (a), EDFA shows no gain because its current is too low at 10%. In contrast, the results in Fig. 8 (b) at 50% current show significant gains. Those smaller input powers on the right-most wavelengths give larger gains; thus, EDFA's gain varies with input power, as concluded in Fig. 5. Notably, this EDFA's noise floor is not flat across C-band due to internal gain equalizer. The noise floor increases with gain and EDFA laser current.

(a) (b)

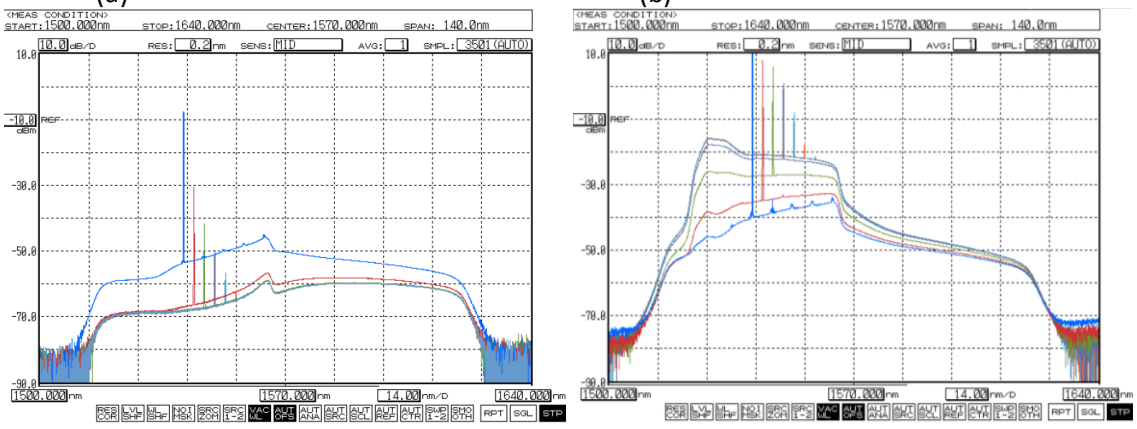

Figure 2 Output spectral profiles of EDFA (VIAVI) at laser current of (a) 10% and (b) 50%

3. Polarization Dependent Loss (PDL): we use a polarization controller to vary the input polarization of EDFA while monitoring output power *P* in Fig. 9 block diagram. The power difference ($P_{max} - P_{min}$) is PDL. Table 1 lists all measurements at 50, 75 and 100% laser currents. This 0.05-dB PDL is insignificant; thus, EDFA is polarization independent.

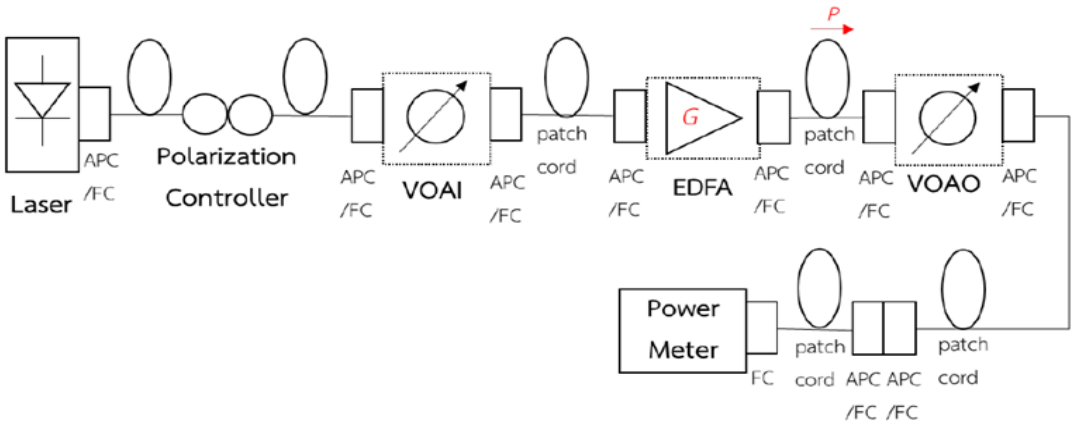

Figure 1 EDFA (VIAVI): Block diagram of PDL measurement

Table 1 EDFA (VIAVI): PDL at different laser currents

EDFA Laser Current (%)	P_{max} (dBm)	P_{min} (dBm)	PDL (dB)
50%	5.88	5.83	0.05
75%	14.51	14.46	0.05
100%	17.13	17.08	0.05

Experimental results of EDFA (Amonics)

1. Gain (dB): as in Fig. 5 block diagram, we use OSA to measure input and output powers of EDFA at 1550 nm wavelength. The gain results in Fig. 10 at 60 and 120 mW laser pump powers are similar to Fig. 5. Clearly, this gain depends on laser power. For example, at P_{in} = -30 dBm, the gain is 27.5 and 30 dB at 60 and 120 mW laser power respectively. Besides, the smaller input power will get a larger gain.

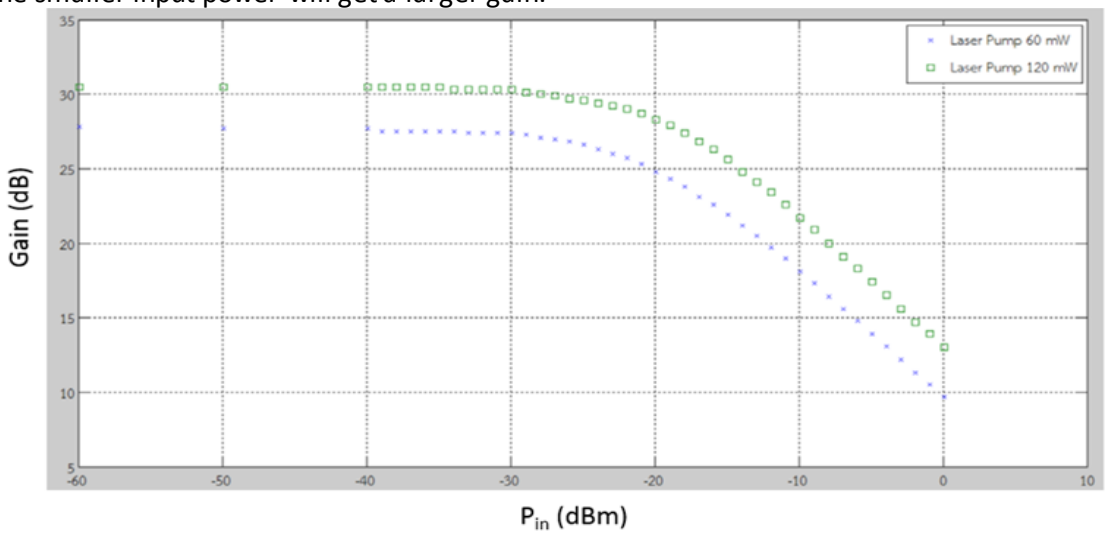

Figure 2 EDFA (Amonics): Gain measurement results

2. Operating Wavelength: as in Fig. 6 block diagram, we measure EDFA's output with no input. Seven spectral profiles are plotted in Fig. 11 at corresponding laser powers: 0, 5, 10, 30, 60, 90 and 120 mW, shown as the bottom noise floor to the highest peak line respectively. Again, the operating wavelength is within C-band from 1528 nm to 1560 nm. Unlike Fig. 6, a longer wavelength than 1560 nm in Fig. 11 shows no gain.

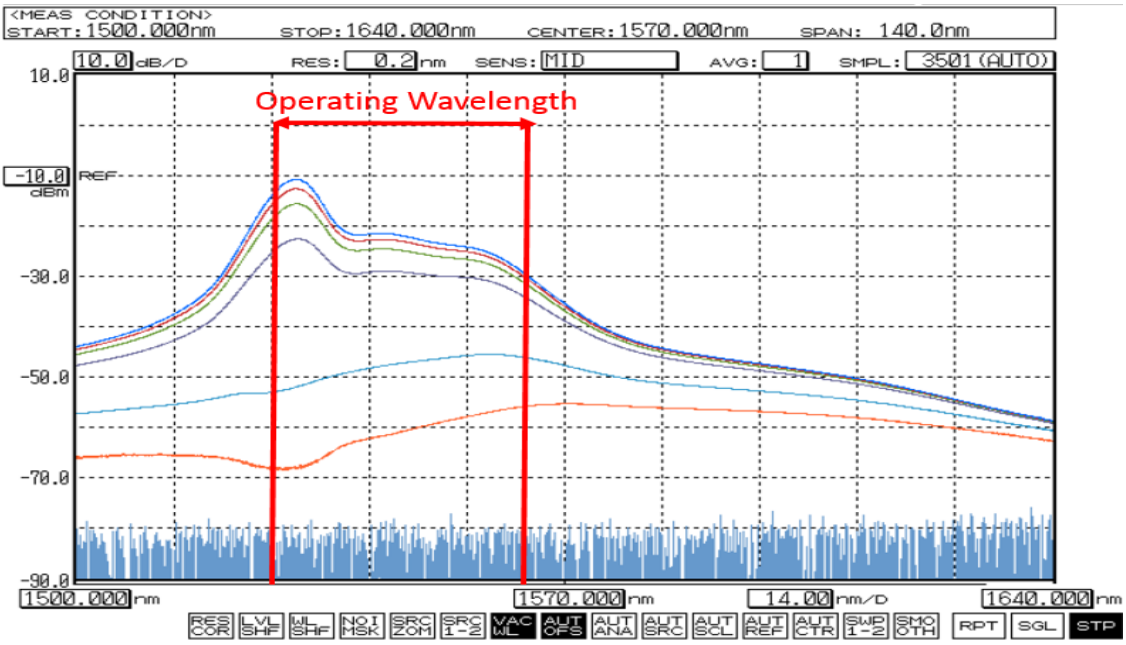

Figure 1 Output spectral profiles of EDFA (Amonics) at different laser powers

Again, we set a tunable laser in Fig. 5 block diagram to output 7 wavelengths: 1540.953, 1543.929, 1549.917, 1549.916, 1552.927, 1555.949 and 1558.983 nm having equal powers as shown in Fig.12 (a), same as in Fig. 7 (a). Next, we attenuate these wavelengths by 5, 10, 20, 30, 40, 50 and 60 dB respectively. Their corresponding spectral profiles are shown in Fig.12 (b) as the input into EDFA.

(a) (b)

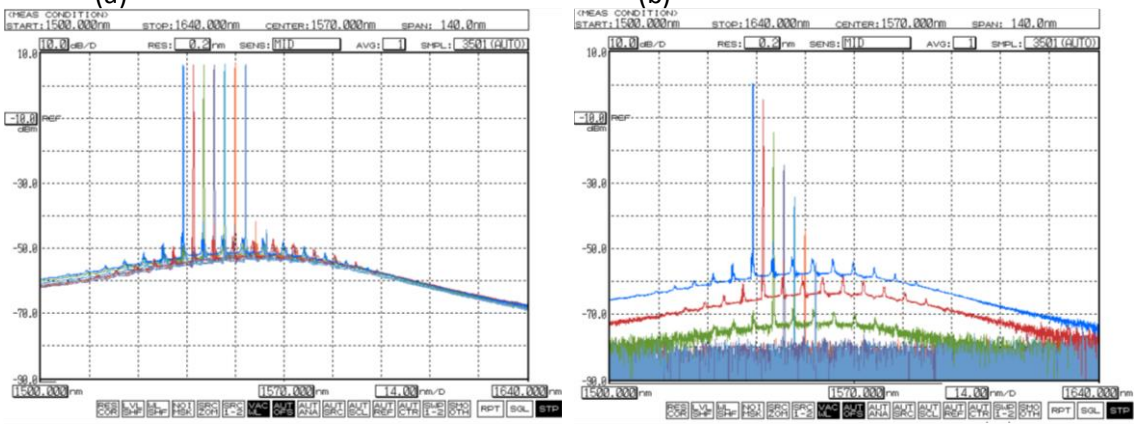

Figure 2 Spectral profiles of 7 input wavelengths: (a) equal powers and (b) attenuated powers into EDFA (Amonics)

The output spectral profiles of EDFA (Amonics) with 7 attenuated input wavelengths are shown in Fig. 13 (a) and (b) at EDFA laser power of 5 and 60 mW respectively. Comparing the results in Fig. 12 (b) and Fig. 13 (a), EDFA shows no gain due to its low power of 5 mW. In contrast, the results in Fig. 13 (b) at 60-mW power show significant gains, similar to Fig. 8 (b). Those smaller input powers on the right-most wavelengths give larger gains; thus, EDFA's gain varies with input power, as already concluded in Fig. 10. Furthermore, the EDFA's noise floor gradually increases with larger gain and higher EDFA laser power.

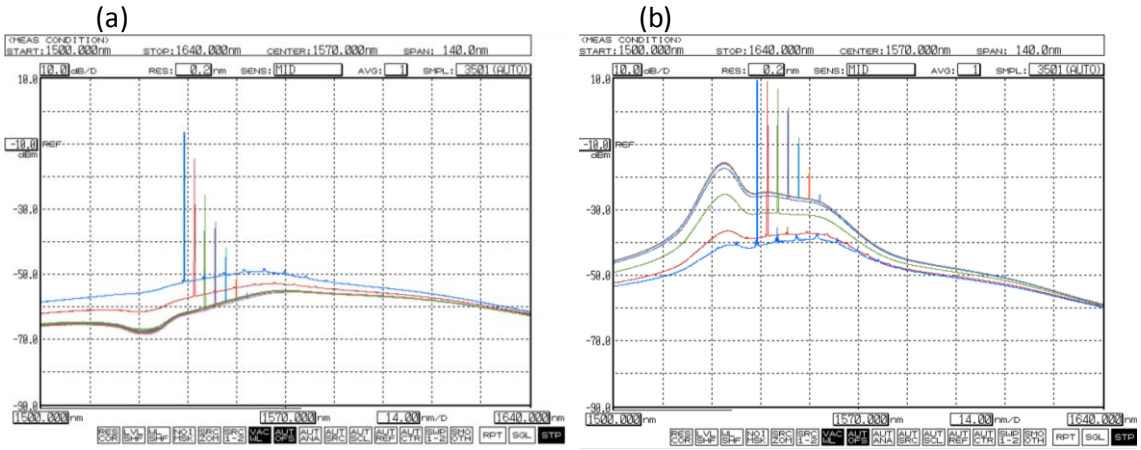

Figure 1 Output spectral profiles of EDFA (Amonics) at laser pump of (a) 5 mW and (b) 60mW

3. Polarization Dependent Loss (PDL): as in Fig. 9 block diagram, we vary EDFA input polarization while monitoring output. The difference ($P_{max} - P_{min}$) is PDL, as shown in Table 2 at 60 and 120 mW laser powers. This 0.2-dB PDL is small, so EDFA is polarization independent.

Table 2 EDFA (Amonics): PDL at different laser powers

EDFA Laser Power (mW)	P_{max} (dBm)	P_{min} (dBm)	PDL (dB)
60 mW	10.1	9.9	0.2
120 mW	13.2	13.0	0.2

Experimental results of SOA (Amonics)

1. Gain (dB): as in Fig. 14 block diagram, we use a polarization controller to vary input polarization of SOA such that the maximum input power (P_{in}, dBm) is obtained at OSA. Then, both input and output (P_{out}, dBm) at 1310 nm wavelength are measured. The gain results are shown in Fig. 14 at midpoint and 15-step right-turn of SOA's current pump. This gain depends on current pump. For example, at P_{in} = -25 dBm, the SOA gain is 19 and 25 dB at midpoint and 15-step right current respectively. Plus, the smaller input power will get a larger gain.

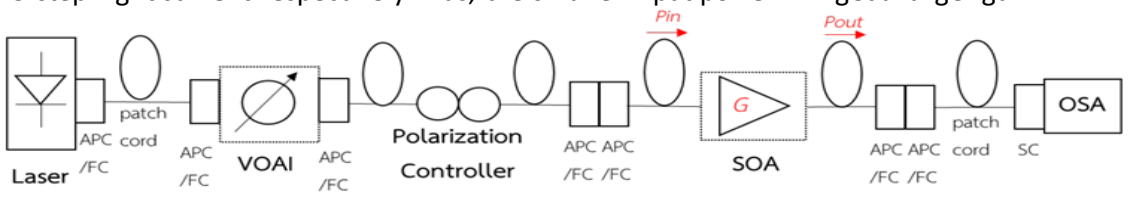

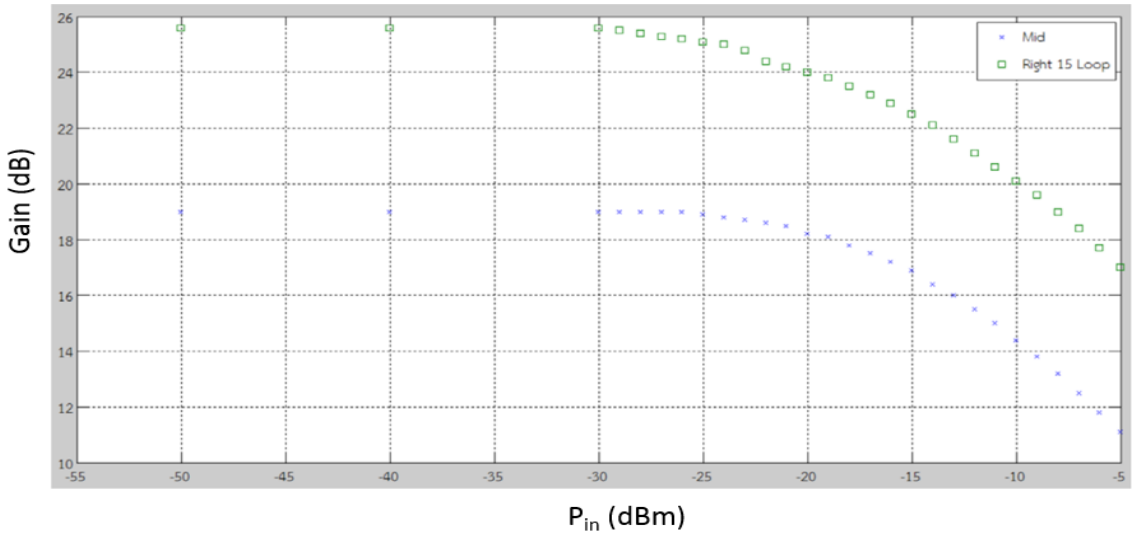

Figure 1 SOA (Amonics): Block diagram of gain measurement and results

2. Operating Wavelength: as in Fig. 14 block diagram, we measure SOA's output with no input laser signal. 7 spectral profiles are plotted in Fig. 15 at corresponding current pumps: 15-step left, 10-step left, 5-step left, center, 5-step right, 10-step right and 15-step right, shown as bottom noise floor to the highest peak line respectively. The operating wavelength is from 1290 nm to 1330 nm, depending on semiconductor dopants.

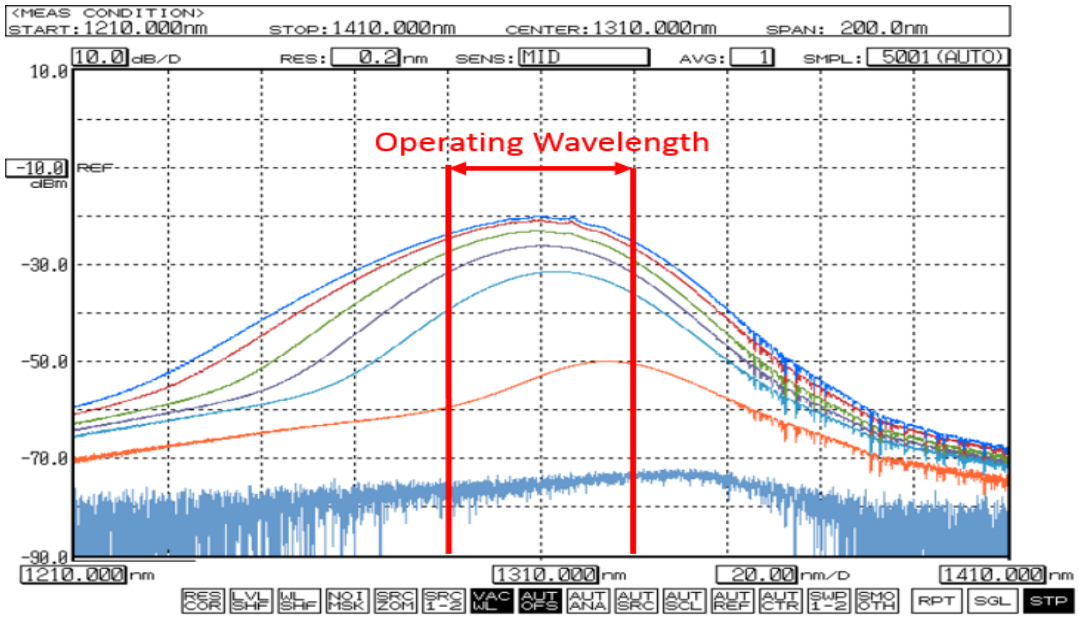

Figure 2 Output spectral profiles of SOA (Amonics) at different pump currents

As in Fig. 14 block diagram, we use OSA to measure input and output spectral profiles of SOA centered at 1310 nm wavelength. Both input and output curve at 15-step right current pump are plotted together in Fig.16 (b). Clearly, the input's noise floor at – 80 dBm rises up to – 25 dBm at SOA output. But, this output's noise floor is below – 20 dBm given in Fig. 15 because there is the laser input of – 5 dBm power into SOA.

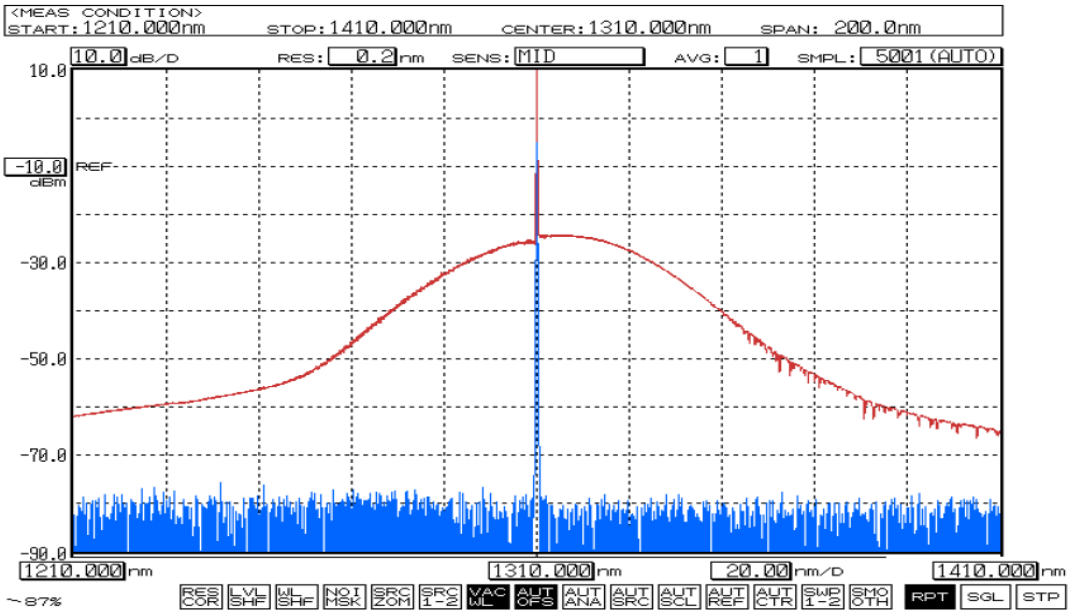

Figure 1 Block diagram and input & output spectral profiles of SOA (Amonics) at 15-step-right current pump

3. Polarization Dependent Loss (PDL): as in Fig. 14 block diagram, we vary SOA input polarization while monitoring its output. The difference ($P_{max} - P_{min}$) is PDL. In Table 3, the PDL are 2.95 and 3.21 dB at center and 15-step right pump currents respectively. These PDLs are extremely high as compared to EDFA, because the SOA is strongly polarization dependent.

Table 3 SOA (Amonics): PDL at different pump currents

Pump Current (Bottom)	P_{max} (dBm)	P_{min} (dBm)	PDL (dB)
Center	5.49	2.54	2.95
15-step right	12.09	8.88	3.21

Next steps of experimental measurements

All experimental results explained above are the characteristic measurements of EDFA and SOA separately. Now, we completely understand the operational conditions as well as the parameters of EDFA and SOA. Next, we will test the bidirectional optical amplifier from NICT as shown in Fig. 17. According to its block diagram, the Downstream (DS) transmission (from right to left) uses an EDFA at 1577 nm wavelength, and the Upstream (US) transmission (from left to right) uses a SOA at 1310 nm wavelength. Finally, the 10 Gb/s access network using this bidirectional optical amplifier will be experimented to measure the power budget and Bit Error Rate (BER) at different combinations of SSMF's lengths and a number of splitting ports.

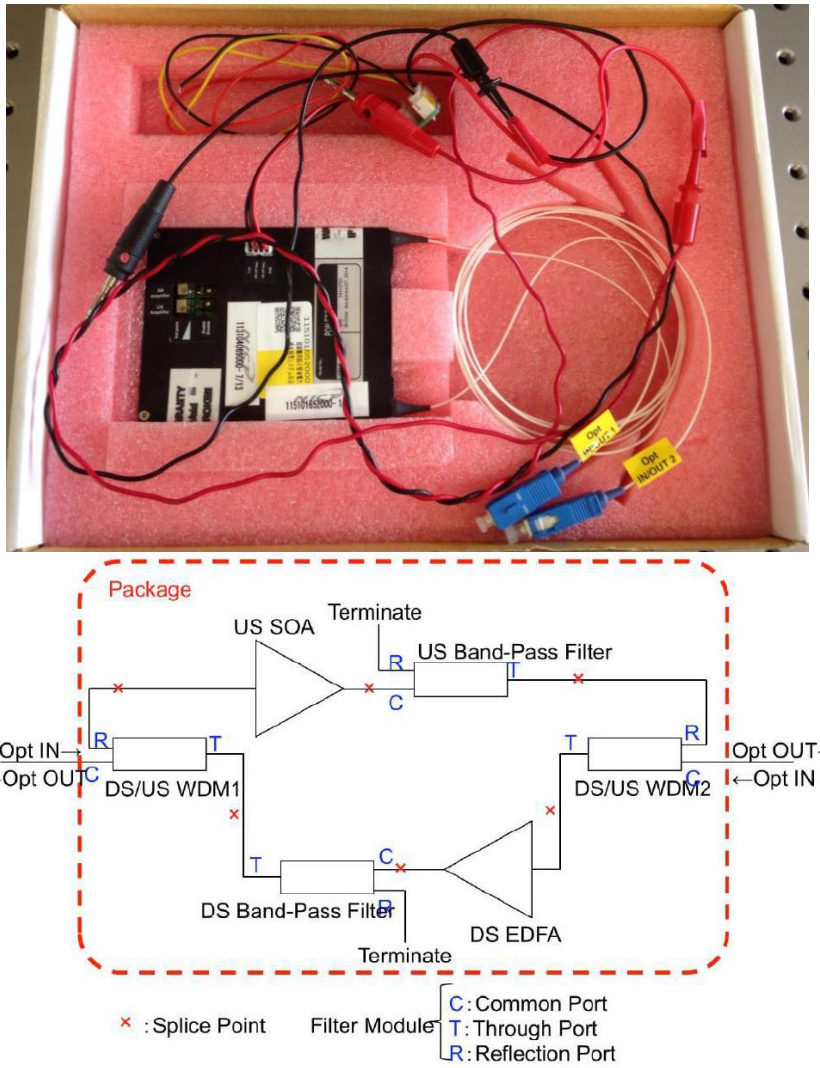

Figure 1 Bidirectional optical amplifier from NICT: photo and block-diagram

Reference

[1] Gerd Keiser, *Optical Fiber Communication*. Singapore: McGraw-Hill, 2010.

[2] ITU Telecommunications Standardization, "ITU-T G.983.3, A broadband optical access system with increased service capability by wavelength allocation," ed, 2001.

[3] ITU Telecommunications Standardization, "ITU-T G.987, 10-Gigabit-capable passive optical network (XG-PON) systems: Definitions, abbreviations and acronyms " in ed, 2012.

[4] ITU Telecommunications Standardization, " ITU-T G.984.2, Gigabit-capable Passive Optical Networks (GPON): Physical Media Dependent (PMD) layer specification," ed.

[5] *SOA Structure*. Available: http://www.fiber-optic-tutorial.com/tag/optical-amplifier

[6] Satoshi Shimizu, Susumu Kinoshita, Ken-Ichi Kitayama, and N. Wada, "0.73-W Extremely Low-Power-Consumption Optical Amplifier Repeater for 10G-EPON Systems," ECOC, 2014.

[7] VIAVI. *mEDFA-A1 Datasheet*. Available: http://www.viavisolutions.com/en-us

[8] Amonics. *C-Band Erbium Doped Fiber Amplifier*. Available: http://www.amonics.com/amonics/php/en/index.php

[9] Amonics. *ASOA13-20-M-FA*. Available: http://www.amonics.com/amonics/php/en/index.php

[10] Yokogawa. *Optical Spectrum Analyzer AQ6370D*. Available: https://www.yokogawa.com/